Optimal Demand Response of Controllable Loads in Isolated Microgrids

by

Akash Raghurajan

A thesis
presented to the University of Waterloo
in fulfillment of the
thesis requirement for the degree of
Master of Applied Science
in
Electrical and Computer Engineering

Waterloo, Ontario, Canada, 2014

Author's Declaration

I hereby declare that I am the sole author of this thesis. This is a true copy of the thesis, including any required final revisions, as accepted by my examiners.

I understand that my thesis may be made electronically available to the public.

Abstract

The electric power industry worldwide has undergone significant changes over the last decade. Environmental compliance and energy conservation issues have occupied the forefront of the new age power system which have opened the possibility of an increased integration of Distribution Energy Resources (DER). With the presence of DERs, reliable system operation and control has become increasingly difficult as the power flow no longer remains unidirectional. Microgrids with their decentralized system operations offer solutions to the challenges posed by this transformation. It has been generally regarded that the key to increased operational efficiency and economy of microgrids especially under its isolated mode of operation lies with improved customer participation in Demand Response (DR) programs. Developing a DR scheme with a novel customer interaction inside a microgrid setup will provide a key solution that would drive the system performance to its peak.

This thesis proposes a mathematical model of DR integrated into the generation scheduling problem of an isolated microgrid. Controllable demand is modeled as a function of external parameters such as outside temperature, Time-of-Use (TOU) pricing and maximum limit on demand P_{max} through supervised learning of neural networks. An optimal DR model is proposed to learn the load behavior and produce a control action on the controllable load profile of the end users. A novel Microgrid Energy Management System (MEMS) is proposed as the central unit of this DR model to determine the control signal and perform a least-cost operational schedule of the microgrid. Realistic data from an actual Energy Hub Management System (EHMS) is used to better replicate the real-world modeling scenario. Continuing with the DR model, the effect of customer response through energy payback model is also studied. The impact of this response on the customer load profile and an estimate of the expected peak reduction is also presented.

The proposed model and the case studies are simulated on an CIGRE IEEE Medium Voltage (MV) benchmark system. The system under consideration is an appropriate approximation of the actual isolated microgrid system with their dispatchable diesel generators, Energy Storage System (ESS), photovoltaic (PV) panels and wind turbines. Finally, the results illustrating the effectiveness of the proposed DR scheme and the computational procedures are discussed. This work is concluded by exploring the possible research directions while addressing some pertinent problems for the same.

Acknowledgements

First and foremost I would like to acknowledge and thank my supervisors, Dr. Kankar Bhattacharya and Dr. Claudio Canizares for their unwavering support and guidance throughout my Masters. Their patience and advice has had an invaluable impact on my student life. I will continue to draw inspiration from you. I would also like to express my thanks to NSERC Smart Microgrid Network for their funding that made this possible.

I would also acknowledge everyone from the Department of Electrical and Computer Engineering for their valuable help during my stay here. I thank all my lab mates for providing me with a peaceful and friendly environment during these two years. A special thanks to Bharatkumar Solanki and Indrajit Das for all the suggestions and guidance. We had some of the greatest discussions that I would always remember. This work would not have been completed if not for the support of Isha Sharma and Felipe Ramos. I would also like to thank Ehsan and Benham for their cooperation.

A very special thanks to Srinivasan for you have been an invaluable friend and mentor to me. Thanks for answering all my questions and introducing me to optimization and computation. My stay at Waterloo has been great fun, the full credits for which goes to Swati. I would also like to wholeheartedly thank my friends Mani, Preetam, Rana, Ankita and Guru. You guys have made each day in waterloo memorable.

Finally, I would like to reserve my special thanks to my family. Your love and belief in me has made me what I am today. I owe everything to you.

Dedication

I dedicate this work to my parents and my sister Preeti.

Contents

List of Figures

LIST OF FIGURES

List of Tables

Nomenclature

Sets

G	Set of generation resources; where G={Diesel, PV, W, ESS}
T	Set of time indices in scheduling horizon

Indices

t	Index for time intervals; where $T \in \{t_1, t_2, \ldots, t_N\}$
g	Index for diesel generators
pv	Index for PV panels
w	Index for wind turbines
ba	Index for ESS
i	Index for neural network input layer neurons
j	Index for neural network hidden layer neurons
l	Index for neural network output layer neurons

Parameters

ax	Fixed cost of diesel generator operation [$]
bx	Diesel generator operating cost [$/kWh]
SUC	Start-up cost of diesel generator [$]
SDC	Shut-down cost of diesel generator [$]
TOU_t	Time-of-use price [$/kWh]
θ_t	Temperature [$^{\circ}C$]
$IW_{j,i}$	Input layer weights of neural network ($\forall \quad j = 1, \ldots, n_H; i = 1, \ldots, n_I$)
$LW_{l,j}$	Layer weights of neural network ($\forall \quad l = 1, \ldots, n_O; j = 1, \ldots, n_H$)
$B_{j,l}$	Input layer bias of neural network ($\forall \quad j = 1, \ldots, n_H; l = 1, \ldots, n_O$)
B_l	Neural network bias at the output neuron ($\forall \quad l = 1, \ldots, n_O$)
n_I	Number of input layer neurons
n_H	Number of hidden layer neurons
n_O	Number of output layer neurons
RU	Ramp up rate [kW/h]
RD	Ramp down rate [kW/h]
UT	Minimum up-time [h]
DT	Minimum down-time [h]
U_g^0	Number of continuous time periods a unit has been on/off at the beginning of scheduling period [h]

$x_{g,t}^{on}$	Number of hours a unit has been in on/off at the end of t [h]
P_{min}^{g}, P_{max}^{g}	Minimum and maximum generation limit of diesel generator [kW]
R_g	Spinning reserve [kW]
$P_{pv,t}$	Photovoltaic output [kW]
$P_{w,t}$	Wind turbine output [kW]
Pd_t^0	Base load profile [kW]
$P_{min}^{ba}, P_{max}^{ba}$	Minimum and maximum dispatch limit of ESS [kW]
$C_{ba}^{min}, C_{ba}^{max}$	Minimum and maximum storage limit of ESS [kWh]
η_{ch}, η_{dch}	Charging and discharging efficiency of ESS
Pd_t	Aggregate system load [kW]

Variables

J	Cost objective function [$]
$P_{g,t}$	Diesel generator output [kWh]
$P_{ch,t}$	ESS output during charging phase [kWh]
$P_{dch,t}$	ESS output during discharge phase [kWh]
$H_{j,t}$	Hidden layer variable corresponding to j^{th} hidden neuron
$a_{j,t}$	Activation variable for j^{th} hidden neuron
Pd_t^e	Neural network controllable demand output for one batch of input [kW]
$SOC_{ba,t}$	State of charge of ESS [kWh]
$Pmax_t$	Controllable demand limit [kW]
$v_{g,t}$	Diesel generator commitment status [1= ON; 0= OFF]
$y_{g,t}$	Start-up decision of diesel generator [1= STARTUP; 0= OTHERWISE]
$z_{g,t}$	Shut-down decision of diesel generator [1= SHUTDOWN; 0= OTHERWISE]
$ch_{ba,t}$	ESS charging decision [1=CHARGING; 0= OTHERWISE]
$dch_{ba,t}$	ESS discharge decision [1=DISCHARGING; 0= OTHERWISE]

Glossary of Terms

DSM	Demand Side Management
DR	Demand Response
FERC	Federal Energy Regulatory Commission
DG	Distributed Generation
ESS	Energy Storage Systems
PV	Photovoltaic
HOEP	Hourly Ontario Energy Price
DER	Distributed Energy Resources
DLC	Direct Load Control
TOU	Time-of-Use
EHMS	Energy Hub Management System
VPP	Virtual Power Plants
HVAC	Heating, Ventilation and Air-Conditioning
RTP	Real Time Pricing
MGO	Microgrid Operator
ISO	Independent System Operator
CHP	Combined Heat and Power
UC	Unit Commitment
AMI	Advanced Metering Infrastructure
MLP	Multilayer Preceptrons
MINLP	Mixed Integer Nonlinear Programming
MILP	Mixed Integer Linear Programming
NLP	Nonlinear Programming
GAMS	General Algebraic Modeling System
LPE	Load Profile Estimator
LPA	Load Profile Aggregator
MEMS	Microgrid Energy Management System
SOC	State of Charge
MSE	Mean Square Error
MV	Medium Voltage

Chapter 1

Introduction

1.1 Motivation

The electric power industry worldwide has undergone significant changes over the last decade. Environmental compliance and energy conservation issues have occupied the forefront of the new age power system which have opened the possibility of an increased integration of Distribution Energy Resources (DER). With the presence of DERs, reliable system operation and control has become increasingly difficult as the power flow no longer remains unidirectional. Microgrids with their decentralized system operations offer solutions to the challenges posed by this transformation. It has been generally regarded that the key to increased operational efficiency and economy of microgrids especially under its isolated mode of operation lies with improved customer participation in Demand Response (DR) programs. Developing a DR scheme with a novel customer interaction inside a microgrid setup will provide a key solution that would drive the system performance to its peak.

DR refers to the change in consumption patterns of end-use customers over time in response to varying price signals. The Federal Energy Regulatory Commission (FERC) of USA has defined DR in [1] as "Changes in electric usage by demand-side resources from their normal consumption patterns in response to changes in the price of electricity over time, or to incentive payments designed to induce lower electricity use at times of high wholesale market prices or when system reliability is jeopardized." The DR programs coupled with increased customer participation and increased decentralization of the system

have been instrumental in enabling Distributed Generation (DG), Energy Storage Systems (ESS) and alternate energy sources such as wind and solar power. These generation resources with DR present a sustainable system with reduced losses and flexible operational characteristics.

The importance of DR and its purported impact on electricity pricing has been succinctly presented in the case study [2]. According to the study, if Ontario market had an additional 250 MW of DR capability when the Hourly Ontario Energy Price (HOEP) was greater than 120 $/MWh, the yearly average price would have been 2% lower, implying a 170 M$ reduction in electricity costs for the customers. This clearly emphasizes the scope for an increased and efficient DR mechanism in Ontario. In another study [3], in the aftermath of the heatwave in northeastern United States and in Ontario, Canada, in 2006, voluntary load reduction on a certain day resulted in an estimated energy payment savings of 230 M$. DR is therefore an important research objective with enormous potential and economical value, and is expected to gain further momentum in the emerging markets in the years to come.

According to Public Act 12-148 of the USA Senate Bill [4] , microgrids have been defined as a group of interconnected loads and DER within a clearly defined electrical boundary that can act as a single controllable entity with respect to the grid or that can alternate between connected and isolated mode of operation. Microgrids can be seen as a small vertically integrated system with generation and distribution components that are capable of providing increased grid resilience and improved reliability. Focus on efficiency, sustainability and reliability have increased the dependency on smart technologies and advanced control, resulting in smart microgrids.

Smart microgrids can be seen as the building blocks of larger unified smart grids and sometimes as a medium of supply to remote areas. In order to justify the system requirements, some features of the smart grids, such as smart meter interface, data security, ESS, DGs, DR and renewable sources of energy [5] have been incorporated into the microgrid architecture. Smart meters along with a reliable communication framework can be used as a means of communication between the utility and the customers. Smart meters could in turn increase customer participation and help in optimizing the system operation [6] by reducing the peak load while considering the customer priorities and flexibilities.

In Canada, research on microgrids are being carried out in several Universities in collaboration with various electric utilities, industries and the stakeholders of DER. The NSERC

Smart Microgrid Network [7], a multi-disciplinary research network, has been instrumental in developing technologies to help Canada in its smart grid transition. Most of the research activities in [7] have been centered around the control/protection strategies, DR based energy management and penetration of DER. In [8], current research activities across various microgrid test beds in Canada have been presented. The core research activities on test beds have been carried out in Ramea wind-diesel system, Fortis-Alberta grid tied system, BCIT test system and a portion of Hydro Quebec distribution system in an effort to understand and improve the microgrid operation.

The advances in DR programs and microgrids have to be sustained to steer the markets and power grids in the right direction. Continuing research activities on DR under the microgrid framework has been the motivation for this work.

1.2 Literature Review

1.2.1 Demand Response

Utilities have long wanted to flatten the load curve in an effort to reduce the production costs and lighten the power system stresses. This has led to different price based and incentive based DR schemes that encourage customers to alter their power consumption patterns in such a way that the social welfare is maximized. In this section, a review of some of the current research works on DR is presented while retaining the focus on incentive and price based DR.

Direct Load Control (DLC) can be classified as a type of incentive based DR scheme where the utility holds a direct control of the customer's load. Loads can be controlled by the operating utility within specified limits to match the available generation at that instant and minimizing the uncontrolled load losses. In [9], Ng *et al.* propose a profit based utility driven DLC arguing that a cost minimization approach results in revenue loss since it does not include customer rate structure. The number of customers to be controlled under the DLC program is considered a decision variable based on price, payback ratio and load pattern. In this research, the customer rate structure via Time-of-Use (TOU) prices is included within the cost minimization objective to capture the response of the customers.

Kurucz *et al.* in [10], investigated DLC from the perspective of peak reduction of the controlled demand, by proposing a strategy with individual control rules on various controllable loads of a residential system. Though, a utility may want to reduce the system demand, a customer participating in a DR program may essentially try to shift the demand based on the customer rate structure, thus keeping a constant total energy consumption. The energy payback model proposed in this thesis, optimally determines the demand shift required from customers across the hours, so as to achieve its operating objectives.

A DLC strategy on Virtual Power Plants (VPP) has been proposed in [11] to implement optimal load control measures for a set of Heating, Ventilation and Air Conditioning (HVAC) devices grouped together as a VPP with an aim to maximize the load reduction over a set control period. In this thesis, the temperature dependent load function concept of [11] has been extended by incorporating customer price structure, thus providing additional dimensionality to implement optimal control measures for all the controllable loads.

Literature on price based DR can be divided into three areas of study. The first line of study is directed at minimizing the customer's electricity payment while ensuring a desired comfort level through price based DR [12]. The second line of work deals with the design of a price based DR scheme to maximize the retailer's profit [13]. The third line of study deals with a DR scheme where a utility and the customer interacts to minimize their respective costs [14]-[16].

In [15], an interface between the electricity market and the customer response from a DR point of view is discussed. A novel concept of 'Homeostatic Utility Control' has been proposed comprising a three stage application- short term load following, Real Time Pricing (RTP) and communication capability. A communication interface to maintain a supply-demand equilibrium, as envisioned in [15], has been proposed in this thesis, between the load estimator and energy management system of the microgrid. The work in [16] proposes to optimally schedule the user appliances by predicting the demand as a function of TOU prices. An adaptive neural-fuzzy learning algorithm is used where the utility determines a differential pricing scheme based on the predicted demand, thus enabling a closed loop interaction between the utility and the customer. A master controller interfacing between the load aggregator and the utility controller, to arrive at an optimal energy management schedule is discussed. The controller receives user preferences, TOU price and other utility data as input and outputs the predicted energy usage at the customer side.

In the present study, a neural network learning technique has been employed to model the controllable load of the customer. Application of a control signal by the Microgrid Operator (MGO) to reduce the effective demand of individual customers has been proposed. This control will be particularly useful from the perspective of an isolated microgrid where neither energy markets nor Independent System Operator (ISO) exist to regulate the real-time prices. Rather, a simpler control of the load is desired. Principles of utility-customer interface, as mentioned in the earlier works, have been envisaged while modeling the optimal DR framework in this work.

1.2.2 Demand Response in Microgrids

The existing energy management systems available to operators will soon seem archaic with the increasing integration of renewable energy sources, DGs, ESS and electric vehicles. With the increased penetration of DERs into the power grid, the power flow no longer remains unidirectional and power system control becomes increasingly complex. Microgrids, with their distributed control, provide a novel alternative and can help transform the existing burdened power system into a smart grid network. The study of DR in microgrids holds the key to the operation of a comparatively larger smart grid system. In [17], the role of DR and its importance in an isolated mode of operation of a microgrid has been summarized. It compares the DR in a conventional grid and argues for its heightened role in a microgrid setup with DER integration.

An energy management system, integrating storage and DR in smart microgrids is proposed in [18]. A two-layer market for DR participation, with a local market for the customer and a global market for microgrid interaction is proposed. Though [18] studies the mirogrid energy management through a market structure, the concept of aggregators and microgrid interaction has been utilized in the present work, in the context of the proposed optimal DR model. A multi-agent based microgrid operation is proposed in [13] to optimize the DR and generation scheduling as part of a two-stage scheduling in day-ahead and real-time market. An interaction between the day-ahead scheduler and the real-time scheduler is proposed to enable the load shifting and load curtailments of controllable loads. Instead of a two-stage scheduling, the model proposed in this thesis performs operations scheduling in real-time based on the controllable loads estimated using neural network and the optimal control signal derived from the DR model.

In [19], hierarchical agents have been used to coordinate DR and DGs in order to minimize the energy costs of residential customers. A grid connected microgrid with user feedback to the control agents, stochastic load and wind power are considered in an effort to strike a balance between the cost and comfort. Customer interaction as described in [19] is incorporated in the proposed optimal DR model, where the user privacy is guarded. Unlike the grid connected microgrid with individual micro Combined Heat and Power (CHP) systems to drive a cost based utilization, centralized generation resources in an isolated microgrid are introduced in this present work. ESS devices are integrated into the system with the same purpose of minimizing the energy consumption cost as in [19].

In [20], an energy management algorithm for residential DR is proposed, wherein, the energy costs and customer load patterns are modeled as Markov chains with unknown transitional probabilities to capture the changing load patterns and energy costs. The work uses reinforcement learning techniques to learn the load behavior of the customers and schedules the energy usage through adaptive learning. In this thesis, a supervised learning technique is used to model the load pattern as against the reinforced learning proposed in [20]. The underlying load pattern is learnt as a function of the observations without relearning the model on a trial and error basis, unlike that in reinforcement learning.

Remote inaccessible areas of Canada have been hampering grid connectivity which has raised serious concerns on power supply reliability and operation losses. Isolated remote microgrids could be a saving grace in such circumstances. There are estimated 300 remote communities in Canada housing around 200,000 people which could be served by a microgrid with better connected and cleaner source of power such as wind turbines and Photovoltaic (PV), in a mix with diesel generation sets, to enhance the reliability. One such work to investigate the need for renewable energy alternatives in remote communities in Northern Ontario, Canada, has been carried out in [21]. The work focuses on the renewable alternatives over the conventional diesel generators in the remote communities and presents optimal renewable energy integration scenarios while considering costs and related constraints.

Research in remote microgrids include investigation of system stability, energy management issues and the integration of wind turbines and ESS. Hatley Bay, Bella Coola, Nemiah Valley, Ramea Island and Kasabonika lake [22] are a few testbeds in Canada that are being used for remote microgird analysis. Testbeds of microgrid systems aid in real-time analysis of their operational behavior and shortcomings. DR and operations of smart

microgrids have been applied on such test-beds to test their practical implications. One such work [23] outlines the BCIT test-bed at Burnbay, British Columbia, Canada. At the BCIT test-bed, research has been carried out to investigate DR and efficient distribution of electricity integrated solutions for alternate sources of energy. In [8], an analysis of another test bed namely Fortis-Alberta distribution system with emphasis on grid connected mode of operation of the microgrid is presented.

Extensive studies on the operational aspects and control of smart microgrids have been reported. DR initiatives have also been studied and efforts are being made to implement them at the microgrid level. The presence of DER in the form of renewable energy sources and ESS have had a two pronged effect on their application. On one hand, DERs introduce a wider net of responsive loads and fast acting generators while on the other they have rendered the establishment of a market structure and generation scheduling difficult. Thus, microgrids, especially under isolated mode of operation, have become increasingly dependent on customer response. In this work, an approach to DR incorporating generation scheduling while modeling the consumption pattern of the customer has been proposed.

1.3 Research Objectives

In view of the literature review and discussions presented in the previous sections, the research objectives of this thesis are outlined as follows:

- Estimate a model that would better illustrate the underlying relationship between the distinct external parameters and a residential load. A neural network based modeling procedure will be adopted to capture the load characteristics. The fundamental pattern of this load profile will be extracted from the data collected through real-time measurements in an Energy Hub Management System (EHMS) enabled house in Ontario by implementing a supervised learning technique. The proposed functional relation will be extrapolated to represent the aggregate load profile in a microgrid.

- Develop a comprehensive operations scheduling model in an isolated microgrid encompassing various DG resources. Wind turbine, conventional diesel, PV panels and ESS will be considered to simulate the realistic operational microgrid system. Considering all the dispatch and operational constraints, the generation resources will be scheduled from the perspective of the MGO.

- Integrate the estimated load model into the operations scheduling model of the microgrid. The optimal control action of the MGO through a variable demand limit imposed on the customer will be determined. In essence, a neural network model will be trained to learn the load behavior and effect a control action, thereby scheduling a least-cost energy usage and hence enabling a novel DR strategy.

- Test the performance of the model by subjecting it to different realistic cases. The soundness of the learning process and the subsequent model estimation will be validated with different physical scenarios. The effect of customer payback under the influence of DR scheme as a case study will also be studied. The quantum of demand reduction and cost analysis with the proposed model will be demonstrated.

1.4 Thesis Organization

This thesis is organized as follows. Chapter 2 establishes the background of this work. A generic mathematical model of generation dispatch and fundamentals of neural networks have been presented. This chapter also discusses the mathematical programming techniques and a summary of the computing tools used in this research. In Chapter 3, the mathematical model of microgrid operations and controllable demand modeling have been presented in detail. This chapter also sets up the integrated neural network-microgrid operations model. Chapter 4 presents the case studies with the model developed in Chapter 3. Effect of MGO imposed control signal on the controllable load profile and the resultant DR with cost savings have been presented using simulations in Chapter 4. In Chapter 5, a summary of the research work is presented and conclusions are drawn. This chapter also identifies possible directions for future research on DR in smart microgrids.

Chapter 2

Background

This chapter presents an overview of the tools and models that form the basis of this thesis. In Section 2.1, a background to DR and microgrids has been presented. This is followed by a brief description of the estimation techniques in Section 2.2. Further, a brief outline of neural networks and its architecture, used for system modeling, are discussed in Section 2.3. In Section 2.4, a brief description of the Unit Commitment (UC) problem and its mathematical model has been laid out. Finally, in Section 2.5, a brief overview of the optimization methods and associated solvers used in this work are described.

2.1 Demand Response and Microgrids

DR programs have costs associated with them and the participation of both the MGO and customers are of utmost importance. A DR program can be subjected to different manifestations to achieve its end objective while retaining the user specifications. DR in its simplest form can have two different alternatives. In the first case, customers reduce their consumption during peak load hours according to an established agreement with the MGO which yields benefits to both the entities. This voluntary reduction in consumption by the customer can reduce the energy costs but may result in increased inconvenience and discomfort to the customers. The second alternative is to shift the load to off-peak hours from the peak hours. In this case, the customer reduces its consumption during peak hours driven by high prices and consumes electricity during lower price hours. This pattern of response does not alter the total energy consumption of the customer but only changes

the load pattern. This is beneficial in terms of operational reliability and reduced dispatch costs from the MGO's perspective and decreased payments by the end user. Different alternatives of the DR program can be outlined [24] as shown below:

1. Incentive Based Programs
   a) Conventional
      i) Direct Load Control
      ii) Interruptible Load Management
   b) Market Based Approaches
      i) Capacity Market
      ii) Ancillary Service Market
      iii) Demand Side Bidding
      iv) Emergency DR
2. Price Based DR
   i) Time-of-Use pricing
   ii) Critical Peak Pricing
   iii) Real Time Pricing

DR initiatives are finding increased participation among the utilities and end users. In FERC's annual report on 'Assessment of Demand Response and Advances Metering' [1]; developments in DR, Advanced Metering Infrastructure (AMI) and smart grid standards have been highlighted and their potential in energy management have been documented. One interesting outcome of the report is shown in Figure. 2.1. The figure shows an increase in the peak reduction potential across all customer classes over a span of six years. The report estimates total peak reduction potential of 55,980 MW across all regions of NERC. The quantum of resources that can be used for energy management suggests the significance of DR in today's grid operation especially during the summer months. To better reflect the system performance and the effect of DR, the present work considers the summer months for system modeling.

Smart grids are electricity networks that can intelligently integrate the operational aspects of generators, distribution centers and end users thereby ensuring a reliable, clean

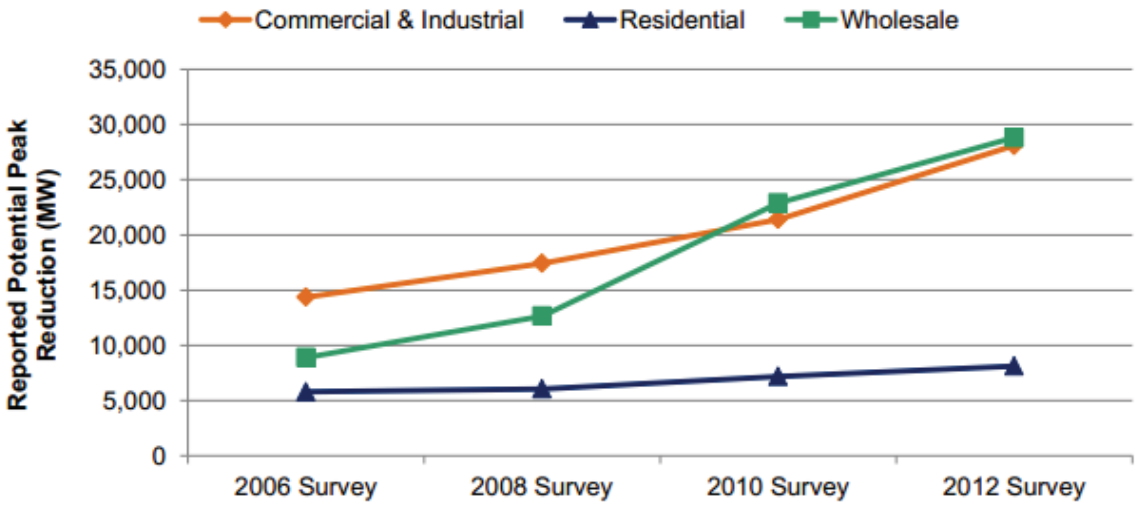

Figure 2.1: Potential peak reduction by customer class [1].

and cost effective supply. The relevance of smart grids in the revision of the current grid infrastructure has been clearly put forth in Grid 2030 vision document [25] of the U.S. Department of Energy. It presents a road map to establish an electric system that could provide abundant, secure and affordable power to every part of the country. Smart grids have felicitated the induction of DG resources like PV panels and fuel cells, the presence of which has divided the power system into smaller islands thereby reducing the losses and improving the sustainability. This has resulted in what is called smart microgrids. A formal definition of microgrids has been presented by the U.S. department of Energy in [26] which states that-" A microgrid is an integrated energy system consisting of interconnected loads and DERs, which as an integrated system, can operate in parallel with the grid or in an intentional island mode." The essential building blocks and the components of microgrids are better illustrated by Figure. 2.2.

Isolated microgrids have been particularly useful in areas where connection to the main grid is restrictive or financially infeasible. In the isolated mode, the system is self-reliant wherein the responsive system load is satisfied by the locally available generation. In the connected mode of operation, the microgrid behaves as a load to the external power system network. The main idea behind this initiative is the drive towards power system reliability, load management and sustainability through its dependency on renewable sources of power. Challenges faced by the isolated microgrids in terms of loss reduction, optimal utilization

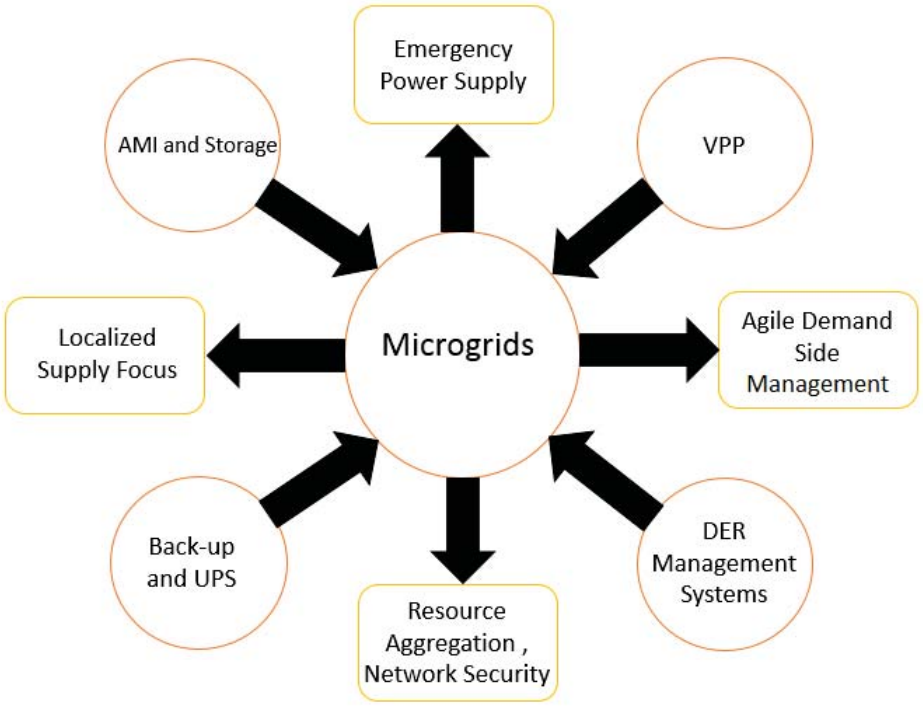

Figure 2.2: Microgrids and their constituents.

of resources, grid stability and security are compounded by the fact that they cannot fall back on a relatively reliable central grid. Efficient energy management systems, AMI and advanced security establishment become the key parameters to enhance reliability in such isolated microgrids. This work proposes an optimal DR scheme on an isolated microgrid, thus augmenting its potential in system operations.

2.2 Estimation and Modeling

Estimation techniques constitute a fundamental block of engineering which help in extracting information from the available data. State estimation and parameter estimation are the two most important branches of estimation theory. State estimation tries to optimally estimate the true state of the system given the system model and the noise induced input. In parameter estimation, the best possible values of parameters are determined with given input and output measurements and boundary conditions. With this brief distinction be-

tween the two broad estimation techniques, a more detailed background on estimation is presented, since it has been used in the modeling techniques in this thesis.

Parameter estimation has been defined in [27] as an inverse problem where discrete measurements of the dependent variables are used to estimate the parameters. The parameters generally define an underlying physical relationship between the distribution of the input and output datasets. This estimation technique is also referred to as nonlinear regression and nonlinear estimation. An estimation function could be better illustrated with the mapping function as shown below:

$$y_i = G(x_i, \theta) \implies y_i = \theta^T x_i + \varepsilon_i \tag{2.1}$$

where y_i is the output, x_i is the input, i is the sample index, θ the parameters to be estimated, ε is the unmodeled error and G is the nonlinear map.

The parameter estimation problem in general falls into two major classes - regression and classification problems. An estimation problem is a classical regression based approach if the input and the output data are continuous in the given domain. Alternatively, it can be grouped into a classification problem if the output of the model takes a limited number of discrete values. Based on the characteristics and assumptions on distribution of the input and output data, few models have been described. The most preliminary but effective model that has been used widely is the linear model. Linear algebraic models tend to provide a fairly simple relation between the input and the output responses. The general linear function and the least square estimation are given as follows [28]:

$$h_\theta(x) = \theta_o + \theta_1 x_1 + \theta_2 x_2 \tag{2.2}$$

$$s(\theta) = \frac{1}{2} \sum_{i=1}^{m} (h_\theta(x_i) - y_i)^2 \tag{2.3}$$

where i is the sample set. The error function shown in (2.3) is minimized with respect to the parameters θ. Maximum likehood estimation are also used to estimate model parameters while incorporating the principles Bayes Theorem.

The linear model as described is used in the context of demand modeling in a microgrid system. It has to be noted that not all loads in a residential unit can be controlled. The controllability over the devices can justifiably be used to reduce the energy cost, consumption, emissions and to even provide a buffer in the form of ancillary service. Thus,

modeling the demand as a function of time dependent internal and external parameters can provide adequate support in smarter control and DR. Once the system is modeled using neural networks by applying the above estimation technique, the optimal system state estimation using optimization is performed.

2.3 Neural Networks

Neural networks can be used to model the complex relation between the input and output parameters using a relatively simple construction and algorithm. One of the main advantages lies in the fact that neural networks have relatively high tolerance limit to noisy data and they have the ability to discern a pattern even for the data that have not been used to train the model initially. An essential characteristic of neural networks is that the correctness of the model output function depends extensively on the goodness of the input data being fed into the model. Thus, learning of the network can be impaired if the input data does not contain sufficient information representing the output.

Neural networks are generally organized in layers with nodes or neurons connecting different layers through an activation function. Data or pattern is presented at the input layer which travels to the hidden layers through weighted connections and is finally processed at the output layer representing the output of the network. As summarized in [29], different neural network structures like Multilayer Preceptrons (MLP), Radial Basis Function and Wavelet Neural Networks have been designed and applied to specific applications. MLP is the most widely used neural network architecture and the same has been applied in this work. In what follows, a brief description of the MLP architecture, its components and training function has been presented.

MLP [30] belongs to a general class of neural networks called feedforward neural networks with one or more layers between the input and the output capable of approximating generic class of functions, including continuous and integrable functions. A general structure of MLP is shown in Figure. 2.3. Here, the first layer is called the input layer. It is a layer which receives a stimulus from outside of the neural network. Every other subsequent layer receives stimuli from its preceding layer. For example, from Figure. 2.3, a layer l receives stimuli from its preceding layer $l-1$. The neurons which receive stimuli from the previous layer's neurons and the output of which is used as a stimuli for outer layer

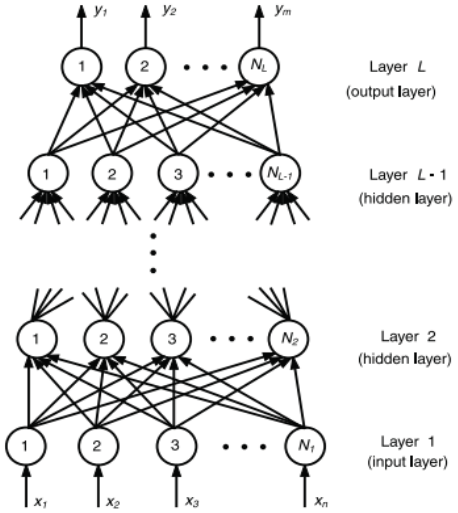

Figure 2.3: MLP architecture [31].

neurons constitute the hidden layer neurons. Neurons, whose outputs are used external to the network are called the output layer neurons. The term stimuli in this context refers to a weighted sum of the inputs passed through an activation function to form an output function. Activation functions are used in the network to scale the data output from a layer. Some commonly used activation functions in neural networks are:

log sigmoid function : The functional representation of the sigmoid function is given below. The function is real valued and differentiable, characterized by horizontal asymptotes as $x \to \pm\infty$

$$\sigma(x) = \frac{1}{1 + e^{-x}} \tag{2.4}$$

$$\sigma(x) = \begin{cases} 0 & \text{when } x \to -\infty \\ 1 & \text{when } x \to \infty \end{cases}$$

where $\sigma(.)$ is the activation function and x is the weighted sum of inputs from the preceding layer.

tan sigmoid function : This function can be represented as

$$\sigma(x) = \frac{2}{1 + e^{-2x}} - 1 \tag{2.5}$$

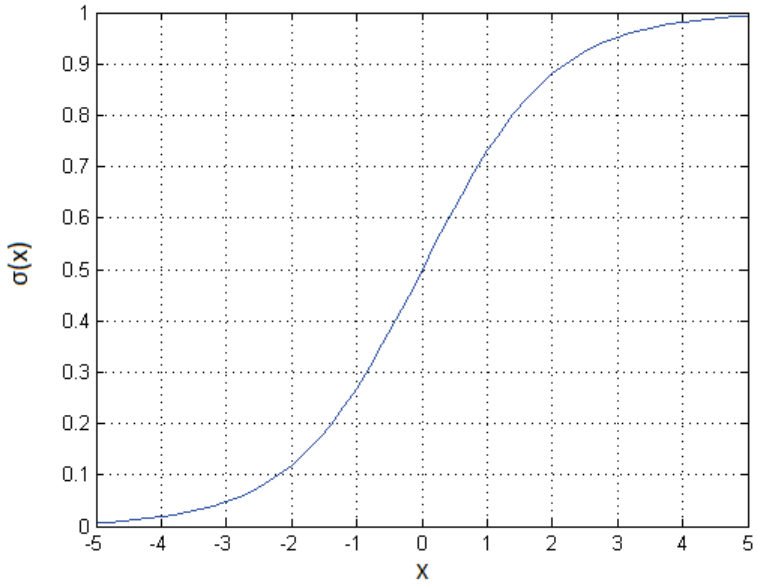

Figure 2.4: log sigmoid function.

$$\sigma(x) = \begin{cases} -1 & \text{when } x \to -\infty \\ 1 & \text{when } x \to \infty \end{cases}$$

This function can alternatively be represented by a hyperbolic tan function as

$$\sigma(x) = \frac{e^x - e^{-x}}{e^x + e^{-x}}. \tag{2.6}$$

The above equation can also be represented as

$$\sigma(x) = \frac{2}{\pi} \arctan(x). \tag{2.7}$$

As stated earlier, input to the activation function is the weighted sum of the response from the previous layer. Suppose, if the response from the preceding layer is null, then the weighted sum of the response becomes zero. To provide a bias against this condition, a bias parameter has to be introduced in the neural network structure. The weighted sum upon the addition of the bias parameter is denoted as [29]:

$$x_i^l = \sum_{j=1}^{N_l - 1} w_{ij}^l z_j^{l-1} + b_i \tag{2.8}$$

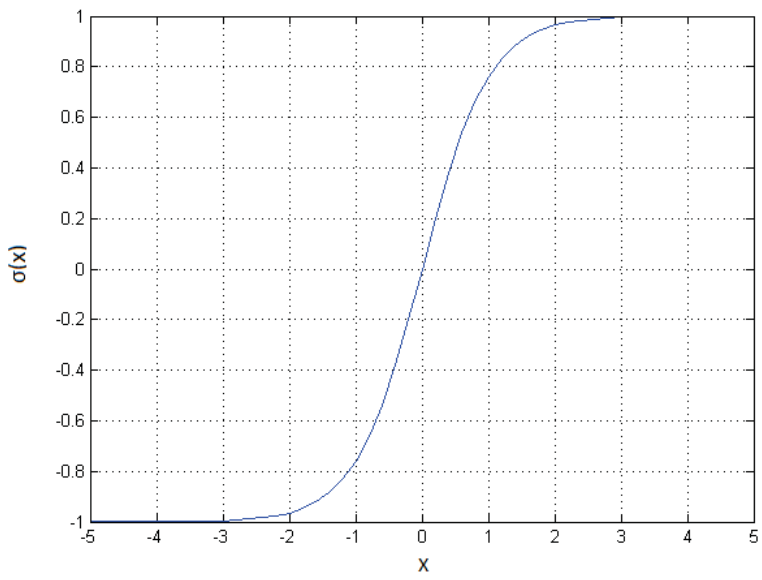

Figure 2.5: tan hyperbolic function.

where $x_i^l = b_i$ represents weighted sum at i^{th} node which is equal to the bias at that node, provided all the previous responses z_j^{l-1} are 0.

Learning in neural network consists of finding the best possible combination of the weights such that a function that provides a best approximation of the original system behavior is obtained. Given input and output patterns, the neural network has to be trained with different pairs of data such that it learns the implicit function that defines the input-output relationship. It optimizes the weights by minimizing the error between the network outputs and the targeted outputs. Given a set (x_p, t_p) of p ordered pairs of inputs and target outputs, the objective is to minimize the error function,

$$E = \frac{1}{2} \sum_{i=1}^{p} \parallel o_i - t_i \parallel^2 . \tag{2.9}$$

Different training algorithms have been developed and currently used in many commercial solvers. Backpropogation of errors using gradient descent algorithm has been one of the most commonly used optimization technique to find the local minima of the above error function. The training algorithm [32] is started by initializing the weights to some small random values and subsequently updating them along the negative direction of the error gradient. Weight is the only parameter which can be changed to minimize the error.

The gradient error function can be calculated as

$$\nabla E = \left(\frac{\partial E}{\partial w_1}, \frac{\partial E}{\partial w_2}, \cdots, \frac{\partial E}{\partial w_i} \right) \tag{2.10}$$

The network weight updates are carried out iteratively using

$$\triangle w_i = -\gamma \frac{\partial E}{\partial w_i} \quad \forall \quad i \in [1, \cdots, p] \tag{2.11}$$

where γ denotes the step length of the iteration and the negative sign indicates a negative gradient. Considering a single input and output network, the algorithm can be summarized in two stages:

• **Feedforward stage** - Input is fed into the network. The network function and its derivative are evaluated and stored at each node.

• **Backpropagation stage** - A constant 1 is fed at the output and the network is run backwards. In this way, the partial derivative of E with respect to weights for each subsequent layer up to the input is computed. The cumulative result is the backpropagated error. Once the derivatives are obtained, the weights are updated by gradient descent
In many commercial solvers including MATLAB ™, $Levenberg-Marquardt$ is the default training algorithm for the feed-forward network due to its robust nature.

According to the universal approximation theorem of the feed-forward neural networks [29], a single hidden layer can approximate any measurable function regardless of the activation function and input space with desired accuracy. Theoretically, there seems to be no constraint on the success of the feed-forward networks. But, it has to be noted that universal approximation theorem does not fix the number of neurons in a layer to guarantee success. In fact, in many black-box models which seldom have any information about the functional relationship and parameters, the number of neurons are selected by trial and error with an objective to minimize the error gradient. A balance has to be struck between an increase in number of neurons of the hidden layer and the convergence rate for a given accuracy, since either of them are directly proportional. Failure to obtain a good model could be attributed to inadequate learning, too few hidden layer neurons or presence of a stochastic relation between the input and output functions.

Once the network has been trained to deduce the weights and biases, it has to be tested and validated to ascertain the quality of the model. Typically, based on the size of the input data set, the data is divided to perform training, testing and validation analysis. Testing of a model is carried out only once against the trained model to obtain the predicted error

using a non-training data. This gives an indication of the performance of the model against an unseen data. Once, the model testing has been completed, the model is subjected to validation tests. A good model is expected to produce a generalized functional relationship between the input and the output. Cross validation of the model is essential to check the generalization of the estimated model. Unlike the test data, the validation data is generally used repeatedly to minimize the non-training performance function such as Mean Square Error (MSE) of the model. Training can be stopped once the validation error performance function stops decreasing or once it reaches the tolerance. Training along with testing and validation concludes the overlying process in developing a neural network model.

2.4 Unit Commitment

The UC problem in power systems is carried out with an aim to optimize the operation of generating resources to supply the load at minimum cost, over a given time period, while satisfying the system constraints. Some of the most widely used methodologies for the solution of UC problems range from integer and linear programming [33], dynamic programming, priority listing, lagrange relaxation, simulated annealing [14], interior point optimization, fuzzy systems and artificial neural networks [16]. A general mathematical model of the UC problem [33] is discussed next.

Objective Function

A simple cost minimization based objective is given as,

$$J = \sum_{t \in T} \sum_{g \in G} C_{g,t}(P_{g,t}) + SU_{g,t} y_{g,t} + SD_{g,t} z_{g,t} \tag{2.12}$$

where the first term of (2.12) represents the generation cost and the second and third terms denote the start-up and shut-down costs, which are usually associated with thermal generators. The cost functions are generally modeled as linear functions while the startup and shutdown costs are typically fixed costs. The objective function is subjected to the following constraints.

Generation Constraint

The generation from generating units are restricted by their maximum and minimum

limits as follows:

$$P_g^{min} v_{g,t} \leq P_{g,t} \leq P_g^{max} v_{g,t} \quad \forall \quad g \in G, \quad \forall \quad t \in T \tag{2.13}$$

Power Balance Constraint

The total generated power should meet the system demand over all time periods under consideration,

$$\sum_{g \in G, t \in T} P_{g,t} v_{g,t} - R_{g,t} = Pd_t \tag{2.14}$$

Ramp up/down Constraints

Limits are imposed on the rate at which generation can increase or decrease. Ramping constraints can be modeled as,

$$\left.\begin{aligned} P_{g,t+1} - P_{g,t} &\leq RU_g \\ P_{g,t} - P_{g,t+1} &\leq RD_g \end{aligned}\right\} \forall \quad g \in G, \quad \forall \quad t \in T \tag{2.15}$$

Minimum Up/Down Time Constraints

A generating unit, especially thermal units, cannot be arbitrarily switched on and off. The operation of the generator is restricted by the minimum time for which it remains on or off which are indicated by the following constraints.

$$\left.\begin{aligned} \left[x_{g,t-1}^{on} - UT_g\right] \left[v_{g,t-1} - v_{g,t}\right] &\geq 0 \\ \left[x_{g,t-1}^{on} - DT_g\right] \left[v_{g,t} - v_{g,t-1}\right] &\leq 0 \end{aligned}\right\} \forall \quad g \in G, \quad \forall \quad t \in T \tag{2.16}$$

The above nonlinear constraints can be linearized as follows,

$$\sum_{t=1}^{L_g} \left[1 - v_{g,t}\right] = 0 \tag{2.17}$$

$$\sum_{i=t}^{t+UT_g-1} v_{g,i} \geq UT_g y_{g,t} \quad \forall \quad t = L_g + 1, \ldots, T - UT_g + 1 \tag{2.18}$$

$$L_g = min\left[T, (UT_g - U_g^0) v_{g,0}\right]$$

$$\sum_{i=t}^{T} \left[v_{g,i} - y_{g,t}\right] \geq 0 \quad \forall \quad t = T - UT(g) + 2, \ldots, T \tag{2.19}$$

where (2.17) ensures that the generating unit will satisfy the minimum up-time constraint if it has been on at hour 0 for fewer hours than minimum up-time. Equation (2.18) ensures the UC status for all sets of consecutive steps of size UT_g. Finally, (2.19) enforces the minimum up-time if the unit has been started at the last $UT_g - 1$ hours. It ensures that the unit remains on for the subsequent hours up to T. On a similar note the corresponding linear form of minimum down-time constraints can be stated as:

$$\sum_{t=1}^{F_g} v_{g,t} = 0 \tag{2.20}$$

$$\sum_{i=t}^{t+DT_g-1} [1 - v_{g,i}] \geq DT_g z_{g,t} \quad \forall \quad t = F_g + 1, \ldots, T - DT_g + 1 \tag{2.21}$$

$$F(g) = min[T, (DT_g - S_g^0)(1 - v_{g,0})]$$

$$\sum_{i=t}^{T} [1 - v_{g,i} - z_{g,t}] \geq 0 \quad \forall \quad t = T - DT_g + 2, \ldots, T \tag{2.22}$$

Equations (2.20), (2.21), (2.22) enforce similar constraints as the minimum up-time except that the UT_g has been replaced by DT_g and start up indicator by shut down alternative.

Coordination Constraints

Relation between start up and shut down decision variables are given as:

$$y_{g,t+1} - z_{g,t+1} = v_{g,t+1} - v_{g,t} \quad \forall \quad g \in G, \quad \forall \quad t \in T \tag{2.23}$$

Similarly a unit can either be start up or shut down at a time instant. To avoid the simultaneous operation of the unit the following constraint is imposed

$$y_{g,t} + z_{g,t} \leq 1 \quad \forall \quad g \in G, \quad \forall \quad t \in T \tag{2.24}$$

$$y_{g,t}, z_{g,t} \in \{0, 1\} \quad \forall \quad g, \quad \forall \quad t$$

Spinning Reserve Constraint

To satisfy the system spinning reserve requirement at all time periods the following constraint is imposed.

$$\sum_{g \in G, t \in T} R_{g,t} v_{g,t} \geq R_t \tag{2.25}$$

2.5 Optimization Methods

The mathematical model used in this work belongs to a class of Mixed Integer Nonlinear Programming problems (MINLP). It is a culmination of Mixed Integer Linear Programming (MILP) and Nonlinear Programming (NLP) subproblems, hence a brief overview of the MILP and NLP problems is given.

A general mathematical form of the MILP optimization problem structure is given as:

$$min \sum_{j=1}^{n} c_j x_j, \tag{2.26}$$

$$subject \quad to \quad \sum_{j=1}^{n} a_{ij} x_j = bi \quad \forall \quad i = 1, 2, \ldots, m \tag{2.27}$$

$$x_j \geq 0 \quad \forall \quad j = 1, 2, \ldots, n \qquad x_j \in \{0, 1\}$$

It is referred to as pure or binary integer problem if all the decision variables are integers, *i.e.,* each variable can take either 0 or 1 as its value. A MILP is an optimization problem [34] wherein some or all of the decision variables are integer values and the objective function and corresponding constraints are linear.

In case of integer programming, many different algorithms are used in practice, ranging from heuristics to linear programming relaxation algorithms like Branch and Bound and cutting plane algorithms [34]. One advantage of the latter methods over the heuristic methods is that they are capable of delivering a feasible if not optimal solution against the possibility of no solution. The Branch and Bound and cutting plane algorithms have been widely applied in many commercial solvers that are used to solve the MILP problems. The Branch and bound is a divide and conquer strategy. They are non-heuristic [35] and they maintain a provable upper and lower bound on the globally optimal objective value. The general idea is to divide the feasible region into sub-partitions and bounding it in an iterative procedure until a ε-suboptimal point is achieved [36].

The NLP optimization problem arises if the objective or at least one of the decision variables is a function of nonlinearity or in other words if the feasible region is determined

by nonlinear constraints. The general mathematical form is given as:

$$\min_x f(x) \tag{2.28}$$

$$subject \quad to \quad g(x) \leq 0 \tag{2.29}$$

$$h(x) = 0 \tag{2.30}$$

$$x \in X$$

Many algorithms have been reported to solve the unconstrained and constrained NLP problems. Newton's method has been the most common method to solve the unconstrained optimization problems. The Newton's method [37] shows a quadratic convergence characteristics, while the steepest descent convergence property depends to a large extent on the size of the step.

The MINLP problems arise with the presence of discrete and continuous variables with nonlinearities in the objective function or constraints. It is a special case which combines both MILP and NLP problems both structurally and in complexity. As with NLP problems, the solution associated with the above mentioned methods depend to a larger extent on the initial starting solution. It is common that a problem with nonlinearities in the constraints may converge at a local optimal solution rather than a global optimal solution. Furthermore, introduction of integer constraints introduces non-convexities to the nonlinear problem which imposes additional burden on resource constraints, thus making MINLP a mathematically hard problem to solve.

2.5.1 Tools and Solvers

In this work, GAMS [38] has been used as a primary tool on which the optimization framework rests. The DICOPT solver [39] has been used for solving the MINLP problem formulated in this work. The algorithm is based on outer approximation, equality relaxation and augmented penalty. The algorithm solves an NLP problem with relaxed integer constraints and stops if this first run yields an integer solution. If no integer solution exists at the first run, the problem is divided into NLP subproblems and an MILP master problem. At the subsequent major iterations, these NLP subproblems are solved for the fixed binary variables predicted by the master problem which finally halts at the instance of a stopping criteria. In this work, optimization of the MILP master problem has been

carried out using the CPLEX [40] solver. CPLEX primarily uses Branch and Bound with cuts and heuristics for solving pure integer and mixed integer programs. To speeden up the operation and to reduce the computational time, several parameters in CPLEX can be fine tuned. The SNOPT solver [41] has been used for solving the nonlinear subproblem. It uses a sparse sequential quadratic programming method to solve constrained optimization problems.

MATLAB ™ [42] has been used to perform the neural network analysis of this work. MATLAB's Neural Network toolbox [32] has a range of functionalities that include function approximation, nonlinear regression, pattern regression, clustering and time series analysis. In this work, a neural network function fitting tool has been used to train the model. MATLAB ™ is efficient in neural network function analysis [32] and it provides many key functions in an effort to arrive at suitably approximated model. Besides numerous training algorithms such as *Levenberg-Marquardt*, one step secant, gradient descent and resilient backpropogation, it also allows the user to define the input-output processing and activation functions. Some essential parameters like minimum gradient, goal, epochs and time are user defined. Random data division, regularization and early stop criteria that produce generalized models are supplemented by data validation criteria that show error histograms, performance plots as a function of epochs and regression analysis. This combined validation results gives us an amply clear picture of the model behavior and response.

2.6 Summary

In this chapter, background of DR and microgrids and its impacts have been discussed. This was followed by a brief analysis of the estimation and modeling techniques. The chapter provided an introduction to the basic definitions and a foundation to the estimation procedures. Neural networks have been used with a specific purpose of functional approximation which in the context of this work refers to load modeling. Neural network feedforward architecture and the backpropagation algorithm were discussed in detail to illustrate the general model of the network. A general mathematical formulation of the UC optimization problem has also been presented. Finally, a brief description of the general optimization methods specific to this work and the associated tools and solvers were presented.

Chapter 3

Modeling Framework for Optimal DR of Controllable Loads

In this chapter, details of the specific mathematical models used in this thesis have been presented. In Section 3.1, the operations planning problem of the microgrid is discussed. First, the overall framework of operations including the load estimation and generation scheduling models are discussed followed by the mathematical models. Demand modeling is discussed in Section 3.2 along with the details on the input parameters and neural network architecture of the modeling process. An account of the neural network performance indices during training and validation with simulated results is also presented. Finally, in Section 3.3, the neural network based load function has been derived and the DR-integrated microgrid operations model is presented.

3.1 Microgrid Operations Model

3.1.1 Overall Framework for Optimal DR

The total energy consumption of a residence though small, can provide a major initiative in load following and DR, when aggregated. From the MGO's perspective, a good model can provide the MGO with an accurate estimate of the demand and help manage its generation resources optimally. In the proposed DR framework, an interface between the residential customers and the MGO is presented. A closed loop optimal DR framework

has been depicted in Figure. 3.1 where individual load profiles of residential customers are estimated and the evaluated aggregated demand of the microgrid is presented to the MGO controller. The MGO can use this aggregated demand and issue a control signal through its energy management system. The proposed framework for optimal DR comprises three main modules (Figure. 3.1), namely, Load Profile Estimator (LPE), Load Profile Aggregator (LPA) and the Microgrid Energy Management System (MEMS).

The LPE module learns the controllable residential load profile based on the input historical temperature, the TOU price and MGO imposed demand limit on the customer. A neural network based supervised learning technique is employed by the LPE to evaluate the load profile (actual) and compare it to the historical controlled load profile (target) data. The LPE module can reside inside a customer's house, and communicate the estimated load profile to the LPA module. The LPA accumulates the demand profile from individual customers and provides the aggregated load profile to the MGO which houses the MEMS. The MEMS provides connectivity to both the LPE and LPA modules and it is regarded as the central unit which performs the optimization within the proposed optimal DR framework.

Besides the aggregated data, the MEMS receives inputs such as the generation capacity of diesel generators and ESS units, the predicted wind and PV generation profiles and DG cost characteristics. A cost minimization based optimal operations scheduling of the microgrid is performed by the MEMS unit, and an optimal control signal P_{max} is determined, which is fed back to the LPE at the customer side. This P_{max} signal, along with the temperature and TOU price data is used to estimate the optimal demand profile. Based on this optimal demand, the MEMS determines the least cost optimal generation schedule of all generation resources in the microgrid system. Thus, a DR scheme in the context of microgrids with a simple control has been proposed while retaining its robustness. The overall architecture of the proposed optimal DR framework is shown in Figure. 3.1.

3.1.2 Microgrid Energy Management System (MEMS) Mathematical Model

In this thesis, only isolated mode of operation for the microgrid has been considered. In Chapter 2, the mathematical model of a generic UC problem has been presented, considering a cost minimization objective. In this chapter, the MEMS operations model for an

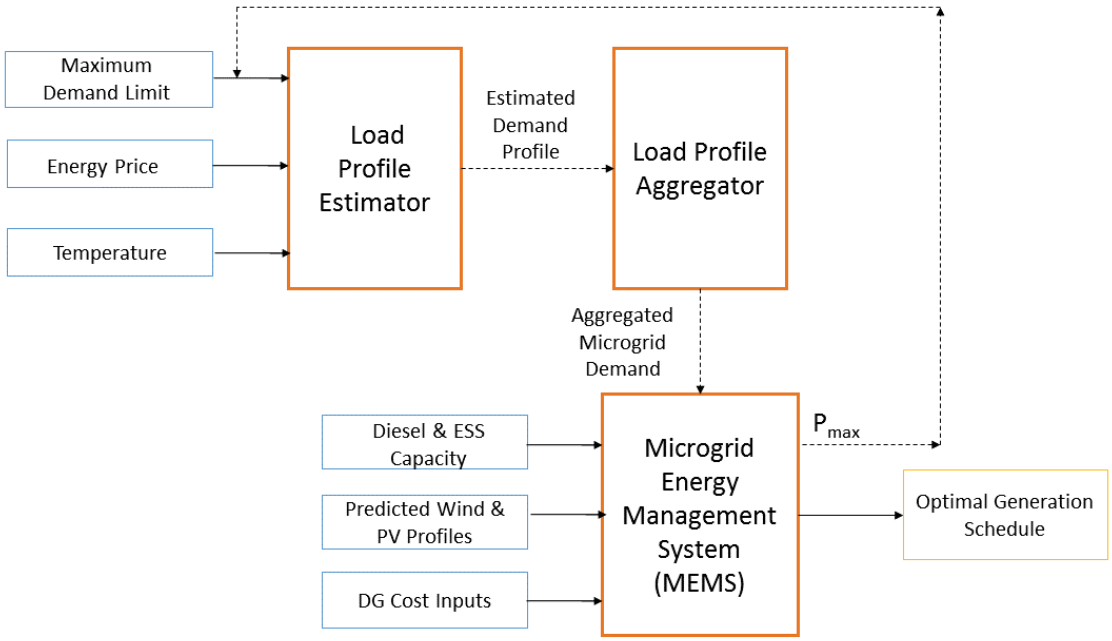

Figure 3.1: Proposed architecture of the optimal DR framework.

isolated microgrid is presented which is based on the UC model discussed in Chapter 2, but with various modifications and some novel features. The microgrid considered, houses a combination of generation resources such as dispatchable diesel generators, PV panels, wind turbines and ESS devices. The objective function (J) given below represents the isolated microgrid operations cost over a scheduling period (typically 24 hours).

$$J = \sum_{g}\sum_{t}(ax_g v_{g,t} + bx_g P_{g,t} + SUC_g y_{g,t} + SDC_g z_{g,t}) + \sum_{ba}\sum_{t}(TOU_t P^{ch}_{ba,t} ch_{ba,t} - TOU_t P^{dch}_{ba,t} dch_{ba,t}) \quad (3.1)$$

where the first term of (3.1) denotes the costs of the dispatchable generators comprising the no-load and operational costs of diesel generators along with their start-up and shut-down costs. The second and the third term accounts for the costs associated with the charging and discharging cycles of the ESS devices. Here, the microgrid gets paid when the ESS is discharging and incurs a cost when ESS is charging. TOU pricing has been used for the ESS devices, so as to align them with customer pricing.

Generation Constraints

The following constraints define the generation limits for the generating sources under consideration.

$$P_g^{min} v_{g,t} \leq P_{g,t} \leq P_g^{max} v_{g,t} \quad \forall \quad g,t \tag{3.2}$$

$$\left.\begin{aligned} P_{ba}^{min} ch_{ba,t} \leq P_{ba,t}^{ch} \leq P_{ba,t}^{max} ch_{ba,t} \\ P_{ba}^{min} dch_{ba,t} \leq P_{ba,t}^{dch} \leq P_{ba}^{max} dch_{ba,t} \end{aligned}\right\} \quad \forall \quad ba,t \tag{3.3}$$

where P^{min}, P^{max} are minimum and the maximum generation capacities of the generating units, $v_{g,t}$ is the binary status variable associated with dispatchable diesel generators and $ch_{ba,t}$, $dch_{ba,t}$ refer to the charging and discharging binary decision variables respectively. $P_{g,t}$, $P_{ba,t}^{ch}$ and $P_{ba,t}^{dch}$ represent the output variables pertaining to diesel generators and ESS devices (charge and discharge) respectively. It is noted that PV and wind generation are considered as exogenous inputs.

Demand-Supply Balance Constraint

The following constraint is used to meet the demand-supply balance at each time period.

$$\sum_g P_{g,t} + \sum_{pv} P_{pv,t} + \sum_w P_{w,t} + \sum_{ba} P_{ba,t}^{dch} = Pd_t + \sum_{ba} P_{ba,t}^{ch} \quad \forall \quad t \tag{3.4}$$

It is to be noted that Pd in (3.4) is the cumulative system load comprising two components, Pd^0 and Pd^e, the base and controllable components respectively, as follows:

$$Pd_t = Pd_t^0 + Pd_t^e \tag{3.5}$$

In the next section, the details of modeling the controllable component Pd_t^e is provided. Equation (3.4) also illustrates that the discharge from ESS is considered a generating source while the charging of the ESS, a load on the microgrid system.

Energy Storage System Constraints

It should be noted that P^{ch} and P^{dch} in (3.3) cannot act simultaneously because a battery can either charge or discharge at a given time instant. Hence, binary decision

variables are introduced within the MEMS model to schedule the operation of the ESS. The operating constraints pertaining to the ESS are as follows:

$$C_{ba}^{min} \leq SOC_{ba,t} \leq C_{ba}^{max} \quad \forall \quad t, ba \tag{3.6}$$

where C_{ba}^{min}, C_{ba}^{max} refer to the minimum and maximum storage limit of the ESS and $SOC_{ba,t}$ signifies the current State of Charge (SOC) of the ESS unit. It also considers that the SOC of the ESS at hour *t+1* is dependent on the SOC at hour t and the charging and discharging powers at hour t. The efficiency of the ESS is assumed to be split between the charging and discharging cycles. The formulation is shown below:

$$P_{ba,t}^{ch}\eta_{ch}ch_{ba,t} - \frac{P_{ba,t}^{dch}}{\eta_{dch}}dch_{ba,t} = SOC_{ba,t+1} - SOC_{ba,t} \quad \forall \quad ba, t \tag{3.7}$$

where η_{ch} and η_{dch} refer to the efficiency under charging and discharging cycles respectively. The complexities introduced by the nonlinearities in (3.7) can be eased by formulating its linear variant using the Big-M method [34]. Accordingly, an implicit either/or relation is obtained as shown by the following equations:

$$\left.\begin{aligned} P_{ba,t}^{ch}\eta_{ch} - M(dch_{ba,t}) \leq SOC_{ba,t+1} - SOC_{ba,t} \\ P_{ba,t}^{ch}\eta_{ch} + M(dch_{ba,t}) \geq SOC_{ba,t+1} - SOC_{ba,t} \end{aligned}\right\} \quad \forall \quad ba, t \neq t_N \tag{3.8}$$

$$\left.\begin{aligned} -\frac{P_{ba,t}^{dch}}{\eta_{dch}} - M(ch_{ba,t} - dch_{ba,t} + 1) \leq SOC_{ba,t+1} - SOC_{ba,t} \\ -\frac{P_{ba,t}^{dch}}{\eta_{dch}} + M(ch_{ba,t} - dch_{ba,t} + 1) \geq SOC_{ba,t+1} - SOC_{ba,t} \end{aligned}\right\} \quad \forall \quad ba, t \neq t_N \tag{3.9}$$

The intuition behind the above equations is that if the ESS is in charging state, SOC_{t+1} is equal to the charging power and SOC_t. The scalar M in (3.8) and (3.9) linearizes (3.7) by imposing one constraint while eliminating the other.

Operational Constraints

These include the ramping and the minimum up/down constraints. The ramping constraints governing the diesel generators can be written as:

$$\left.\begin{aligned} P_{g,t} - P_{g,t-1} \leq RU(1 - y_{g,t}) + P_g^{min}y_{g,t} \\ P_{g,t-1} - P_{g,t} \leq RD(1 - z_{g,t}) + P_g^{min}z_{g,t} \end{aligned}\right\} \quad \forall \quad g, t \neq t_1 \tag{3.10}$$

where RU, RD are the ramp-up and ramp-down rates of the diesel generators and $y_{g,t}$, $z_{g,t}$ refer to the start-up and shut-down binary decision variables. Minimum up/down time constraints, which have not been exclusively shown here, are similar in formulation as in Section 2.4.

Coordination Constraints

It coordinates the start-up and shut-down decisions of the generating units. Relations between the binary decision variables of dispatchable generators and the ESS are given as follows:

$$y_{g,t} - z_{g,t} = v_{g,t} - v_{g,t-1} \tag{3.11}$$

$$ch_{ba,t} + dch_{ba,t} \leq 1 \tag{3.12}$$

$$y_{g,t}, s_{g,t}, v_{g,t}, ch_{ba,t}, dch_{ba,t} \in \{0, 1\}$$

3.2 Load Profile Estimation

In this section, the controllable component of electricity consumption profile of a residential energy hub is modeled considering the parameters influencing this load. In microgrids especially under the isolated mode of operation, responsiveness of every individual load is important. The EHMS in these houses can use the demand data and provide an array of control and operational decisions as a function of related parameters. Using neural network learning technique, the controllable load is modeled as a function of the temperature, TOU prices and the MGO imposed maximum power limit. The training data of neural network is summarized as:

Output Training Data

- System demand-Pd^e (kW): It is the cumulative controllable load on the microgrid arising from the power demand measured from the appliances at a particular time instant. The data is measured with a sampling period of 5 minutes over a time horizon of 24 hours, for a three month period, May to July 2012, providing a total of 288 samples per day. Load measurements are initially carried out considering a particular set value of P_{max}, thereafter, different P_{max} values are assigned and the controlled load profile (target) is simulated.

Input Training Data

- Temperature-T ($^{\circ}C$): The external temperature has an effect on the controllable load component of a residential unit. Therefore, to increase the accuracy of modeling, temperature has been considered over the same time period and granularity as in output.

- Maximum power limit-P_{max} (kW): This limit on the maximum power consumption of a residential energy hub is imposed, as determined by the MGO. Different P_{max} are considered including - 19.5 kW, 6.825 kW, 4.88 kW, 4.8 kW, 2.68 kW, 2.6 kW and 2.55 kW, and for each case the load profile (target) has been simulated.

- TOU price ($\$/kWh$): It is the pricing scheme that had been applicable to residential customers in Ontario. Summer pricing, which corresponds to the pricing scheme in force from May-October, has been used in the proposed optimal DR model. The TOU pricing, which is categorized into off-peak, mid-peak and on-peak based on different times of the day is further subdivided into 5 minute intervals to align with the sampling rate of the measured demand.

Thus, a sufficiently large and unique dataset is presented to the neural network with an aim to produce a fitting network with reasonably accurate function capturing the relationship between output and input. Before feeding the collected data to train the feedforward multilayer network, the data is preprocessed. At the preprocessing stage, constant rows in inputs/outputs are removed since these redundant data do not contribute to the learning procedure. In the next stage, the dataset is normalized within a specific range of [-1, 1] such that the activation function does not saturate. As seen from Figure. 2.5, for large input values the activation function output saturates, resulting in smaller gradients and slower training. Without this step, the training step would have fixed lower weights and biases at the first layer to avoid saturation. The above mentioned steps need be applied again to the targets after training to revert the output back to its original scale. The normalizing function used in this work is given as:

$$y = \frac{(y_{max} - y_{min})(x - x_{min})}{x_{max} - x_{min}} + y_{min} \tag{3.13}$$

where y_{max}, y_{min} take up the values 1 and -1 respectively; x_{max}, x_{min} denote the maximum and minimum values of the input range while x denotes the corresponding input data point.

The input data to the neural network is divided randomly into training, validation and testing datasets in the ratio of $0.7 : 0.15 : 0.15$. Theoretically, there is no limit to the number of hidden layers. Generally, one layer and utmost two layers are sufficient to approximate complex functions. As mentioned in [29], single layer MLP networks are universal approximators. Hence, a single hidden layer MLP is chosen. Number of hidden layer nodes depend on the dimensionality of input and output vectors and also on the training cases. Here, the number of hidden nodes have been determined by comparison of different sets of trained models. Model comparison rests on the fact that, less number of hidden nodes produce high training error and possible under-fitting, while large number of hidden nodes produce over-generalization and subsequent over-trained models. Four hidden neurons have been used in this work after a comparative analysis with other architectures. The adopted neural network architecture is depicted in Figure. 3.2, where $In1 - In3$ represent the three inputs, $IW_{j,i}$ refer to the input layer weights of the network, $LW_{l,j}$ are the layer weights, H_j represents the j^{th} hidden node, B is the hidden node and output node bias and OUT is the output neuron.

As the network is presented with data, weights and biases are initialized and the network is trained in MATLAB ^{TM} platform [42]. Levenberg-Marquardt training algorithm has been used to train the model. The MSE performance function given in (2.9) is used to fine tune the weights and biases in an effort to optimize the model performance. The training algorithm and the stopping criteria, as described in Section 2.3, is applied to the modeling procedure. The network performance and training states are shown in Figure. 3.3 and Figure. 3.4 respectively.

Figure 3.3 shows the MSE for all datasets on a logarithmic scale as a function of epochs; where epoch refers to the number of training trials. Validation and test performance are the points of interest, and the plot shows the iteration at which the validation performance function reaches minimum even as the training is continued for 7 more epochs. Best validation performance has been depicted in Figure. 3.3 which corresponds to an MSE=0.66793.

Figure 3.4 comprises three subplots; the first subplot is the backpropagation gradient expressed in logarithmic scale. It shows the gradient descent across the iterations and arrives at a gradient value of 0.008838 at epoch 39 where the training has stopped. The

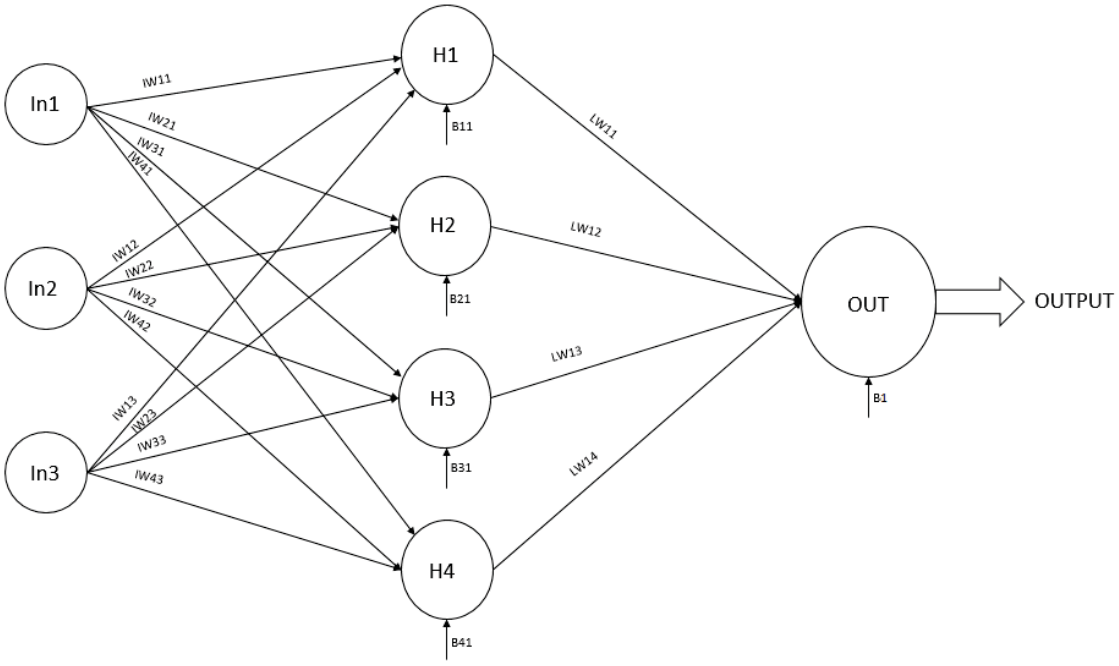

Figure 3.2: Neural network architecture.

second subplot shows the scalar μ dynamics across the epochs; where μ corresponds to the scalar in the Levenberg-Marquardt algorithm at the update step. A small value of μ leads to Newton's method, while a larger μ leads to gradient descent method. This scalar value is decreased when the performance function decreases resulting in a faster and accurate Newton's method. The value of μ increases when the performance function is expected to increase, thus switching to gradient method as the minimum error is far. At the stopping condition, the scalar magnitude is 10. The third subplot shows the validation failure count. As it can be seen at epoch 39, the stipulated count of maximum number of validation fail is reached and the training has stopped.

At the end of the training procedure, it is prerogative to compare the actual model ouput with the target system output. In the study, a total of 84,960 samples are considered. In order to illustrate the fit unambiguously, 600 data points of the two sets are shown in Figure. 3.5.

The neural network inherently subjects the trained model with test and validation datasets to evaluate its flexibility and outputs the best validation performance model. Randomness can be introduced into this model to visualize the model behavior under

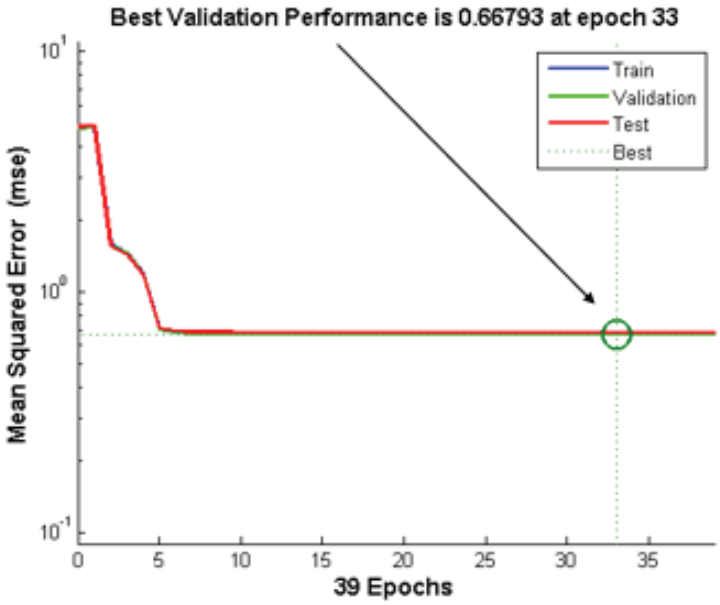

Figure 3.3: Neural network performance plot.

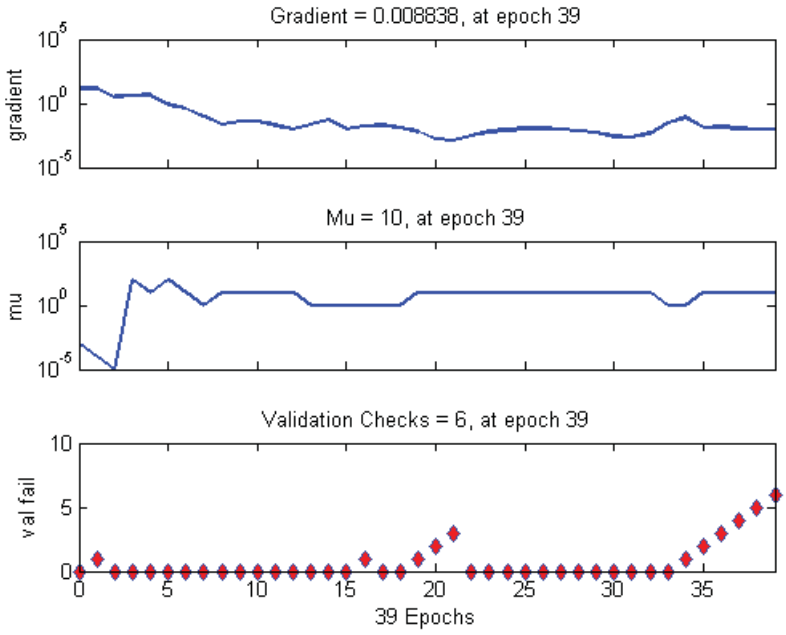

Figure 3.4: Training state plot.

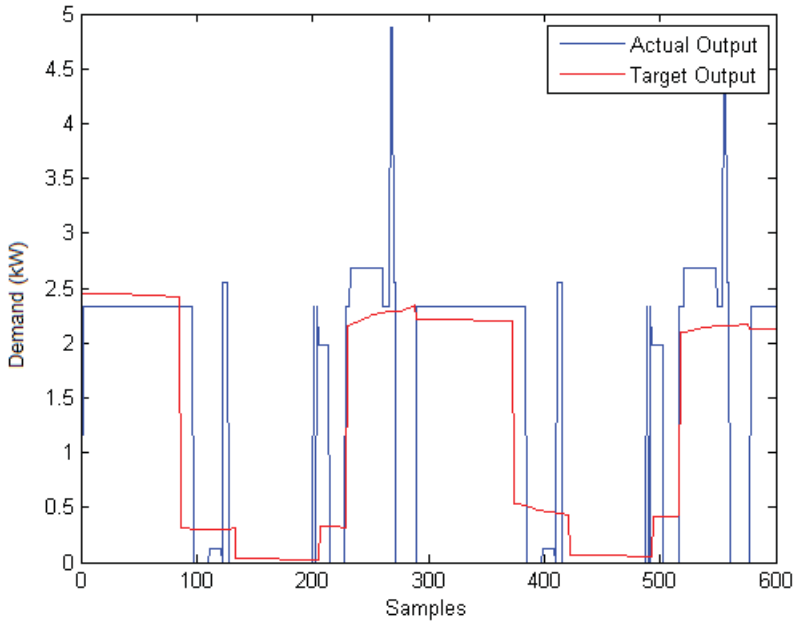

Figure 3.5: Actual vs target output.

constrained random data. In this case, the model is subjected to uniformly distributed random in [0,1] data at the input and the estimated target output obtained has been plotted in Figure. 3.6. It is noted that with constrained random input data i.e., noise, the neural network performance is not deteriorated and thus indicates a fair degree of robustness.

Histograms showing the difference between the actual and the target output is plotted in Figure. 3.7, and as noted, among the total samples considered, majority of the errors lie in the range of -0.44 to 0.62.

Figure 3.8 plots the regression relation between the actual output and the targets. The sampled output is essentially a binary signal in a sense that it has a fixed amplitude touching zero over few alternating sample sizes. The neural network reproduces this behavior in the actual output and in the process the network output lags as the target output shifts. This can be seen from the regression plot (Figure. 3.8) as well as in Figure. 3.5.

After the neural network is trained and validated, the function approximating the input-output relation is extracted. This relation is a function of the network's input weights, layer weights and network biases. The *tan sigmoid* function described in (2.5) is used as the

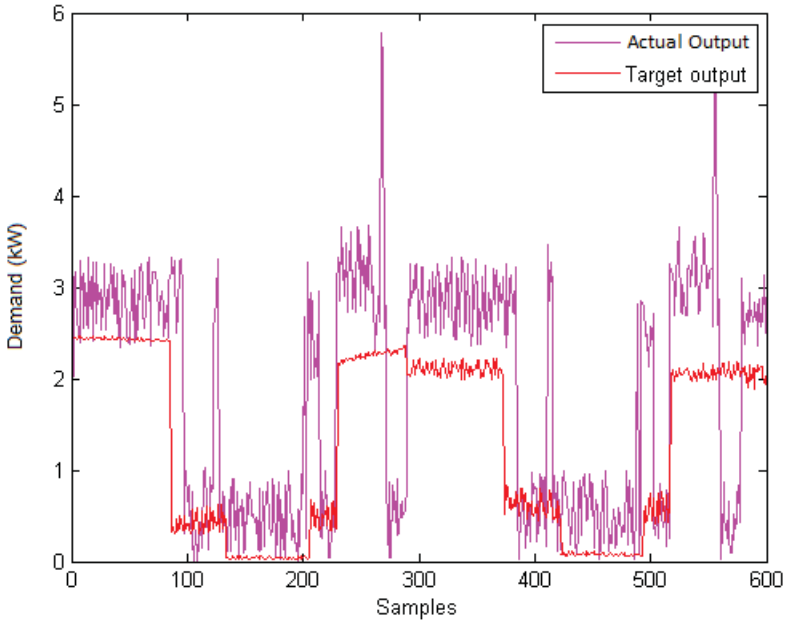

Figure 3.6: Model behavior under random input data.

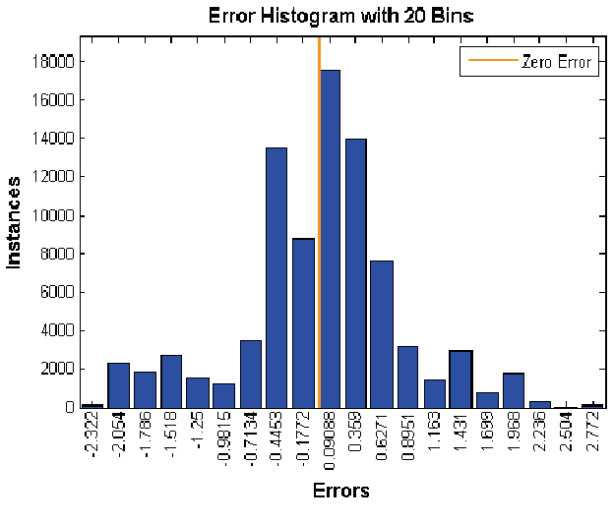

Figure 3.7: Error histogram.

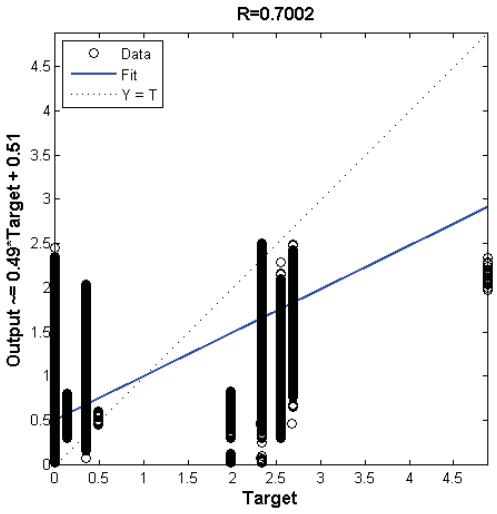

Figure 3.8: Regression plot.

input layer activation function and a linear function is used as the output layer activation function. The weights and biases used in Figure. 3.2 are employed in the respective equations. The mathematical representation of the controllable load function is given as:

$$Pd_t^e = (a_{1t}LW_{11} + a_{2t}LW_{12} + a_{3t}LW_{13} + a_{4t}LW_{14} + B_1) \tag{3.14}$$

where the activation functions a_{1t}, a_{2t}, a_{3t} and a_{4t} are given as:

$$a_{1t} = \frac{2}{1 + e^{(-2H_{1t})}} - 1 \tag{3.15}$$

$$a_{2t} = \frac{2}{1 + e^{(-2H_{2t})}} - 1 \tag{3.16}$$

$$a_{3t} = \frac{2}{1 + e^{(-2H_{3t})}} - 1 \tag{3.17}$$

$$a_{4t} = \frac{2}{1 + e^{(-2H_{4t})}} - 1 \tag{3.18}$$

and the hidden layer function are:

$$\begin{aligned} H_{1t} &= (IW_{11}\theta_t + IW_{12}Pmax_t + IW_{13}TOU_t + B_{11}) \\ H_{2t} &= (IW_{21}\theta_t + IW_{22}Pmax_t + IW_{23}TOU_t + B_{21}) \\ H_{3t} &= (IW_{31}\theta_t + IW_{32}Pmax_t + IW_{33}TOU_t + B_{31}) \\ H_{4t} &= (IW_{41}\theta_t + IW_{42}Pmax_t + IW_{43}TOU_t + B_{41}) \end{aligned} \tag{3.19}$$

where θ_t and TOU_t are the known parameters of measured outside temperature and TOU prices respectively. $Pmax_t$ and Pd_t^e are the variable demand limit and the controllable load estimated by the neural network model respectively.

3.3 Neural Network-Microgrid Integration

For the DR, the controllable demand of the microgrid is the output derived from the neural network function. Given the load model of a microgrid, a control signal p_{max} is determined that optimally schedules the energy while minimizing the operating cost of the MGO. The control signal P_{max} imposes a cap on the peak load from the perspective of the MGO. The controllable demand, which is a function of the temperature, TOU price and P_{max} is the outcome of the optimal DR model.

Parameter estimation of the load model is followed by the microgrid system optimization to simultaneously determine the MGO's control signal P_{max} and the controlled demand

profile of the customers. In essence, P_{max} and the controllable load are deduced at every time instance with varying temperature and TOU price data. The controllable load (Pd_t^e) is integrated into the MEMS model of the microgrid to optimally schedule the generation resources. The resultant MINLP problem has the following representation for the load balance constraint in addition to the previously described MILP problem of UC in Section 3.1.

The demand supply balance constraint of the UC described in (3.4) is replaced by the following to incorporate the controlled load:

$$\left(\sum_{g} P_{g,t} + \sum_{pv} P_{pv,t} + \sum_{w} P_{w,t} + \sum_{ba} P_{ba,t}^{dch}\right) = \left(Pd_t^e + \sum_{ba} P_{ba,t}^{ch} + Pd_t^0\right) \quad \forall \quad t \quad (3.20)$$

where Pd_t^0 is the base load profile across the time horizon that remains unaffected by the temperature and TOU price variations, and Pd_t^e is given by (3.14).

3.4 Summary

In this chapter, a comprehensive mathematical model of UC encompassing all the generation and storage components of a microgrid was presented. Neural network based supervised learning technique has been described in detail to model the controllable demand of th microgrid. Finally, the controllable demand function is extracted from the neural network model and integrated into the MEMS model of the microgrid resulting in an optimal DR scheme.

Chapter 4

Case Studies

4.1 Introduction

In this chapter, the mathematical models developed in the previous chapter are applied to a test case microgrid system to examine the effectiveness of the DR model. In Section 4.2, the microgrid test system and the generation data are introduced. In Section 4.3, simulation cases for the analyses are presented and supported with detailed results and discussions. Finally, in Section 4.4, the computational performance of the proposed model is discussed.

4.2 Microgrid Test System

The CIGRE / IEEE Medium Voltage (MV) benchmark system [43] with DG integration has been used in this work. The 13-bus modified MV rural distribution is shown in Figure. 4.1. The microgrid benchmark system, derived from a German MV distribution network, has a voltage level of 20 kV, supplied by a 110 kV/20 kV transformer sub-station.

As seen in Figure. 4.1, the switch at bus 1 allows the microgrid to alternate between grid connected and isolated modes of operation. In the grid connected mode, bus 1 is modeled as an infinite bus. In this work however, only isolated mode of operation of the microgrid has been studied and the DG unit at bus 1 acts as the main source of reliable power supply. The network parameters and load characteristics used in this work have been

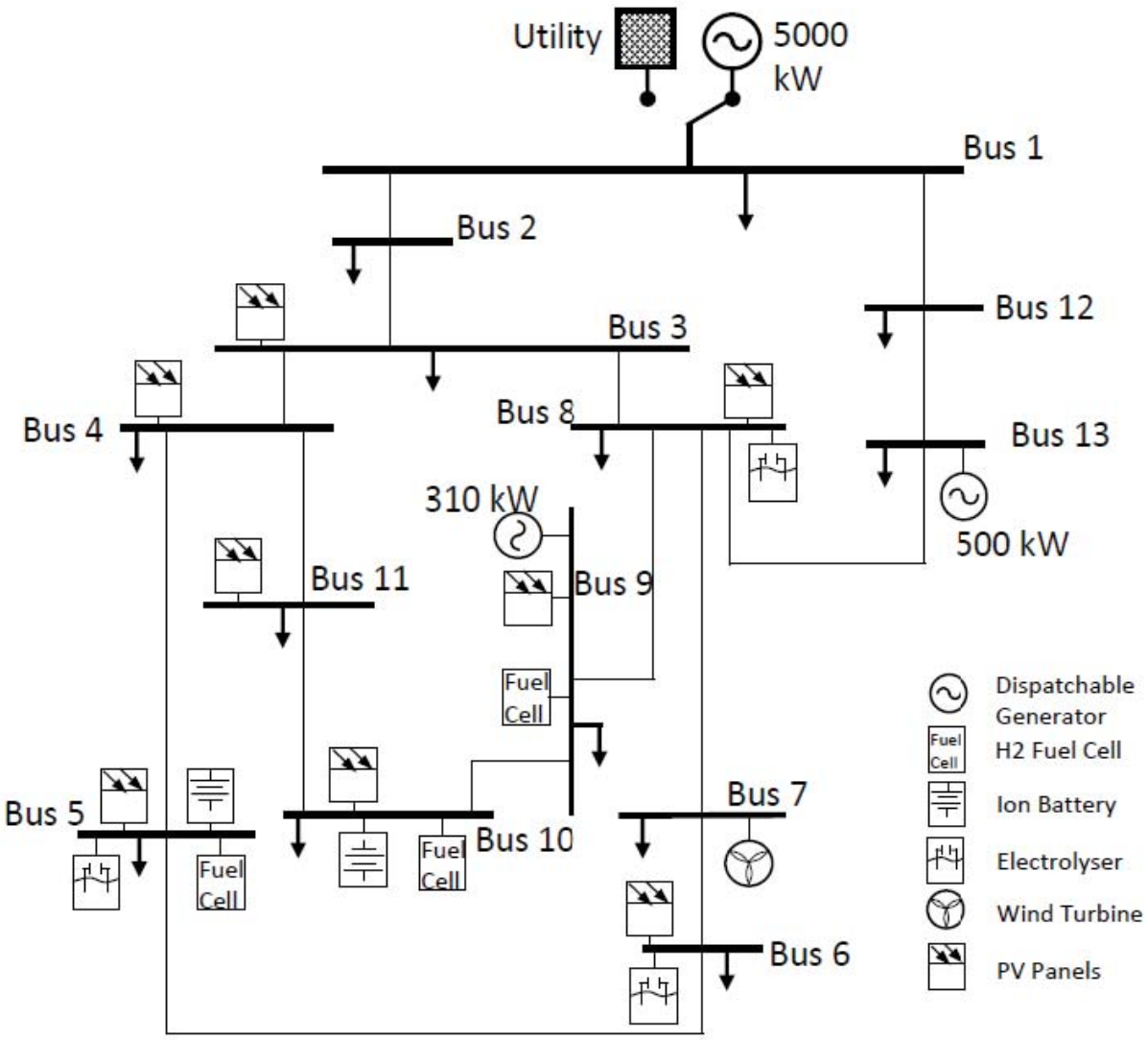

Figure 4.1: Modified microgrid test system.

adapted from [43]. The details of the DG parameters and their corresponding generation capacity are given in Table 4.1.

Table 4.1: Microgrid DER capacity.

Node	Unit	Capacity (kW)
1	Diesel	5000
3	Photovoltaic	20
4	Photovoltaic	20
5	Battery	600
5	Fuel Cell	33
5	Electrolyser	30
5	Photovoltaic	30
6	Electrolyser	50
6	Photovoltaic	30
7	Wind Farm	1500
8	Electrolyser	200
8	Photovoltaic	30
9	CHP Diesel	310
9	Fuel Cell	212
9	Photovoltaic	30
10	Battery	200
10	Fuel Cell	14
10	Photovoltaic	40
11	Photovoltaic	10
13	Gas	500

Temperature and summer TOU pricing data corresponding to the three months from May-July 2012 in the region of Ontario is used in this work. The maximum demand that can be controlled at any instant is approximately 30% of the total fixed base load on the system.

4.3 Results and Discussions

4.3.1 Description of Case Studies

The mathematical model described in the previous chapter has been tested on the microgrid test system considering two different cases:

Case-1: With Uncontrolled Loads

- In this case, the MGO control signal P_{max} is suppressed. In other words, the control signal P_{max} is fixed at its maximum limit and the uncontrolled load is modeled as a function of the exogenous parameters, TOU price and outside temperature only. Therefore, the customer load cannot be controlled by any external signal and this case represents a case without DR.

Case-2: With Controllable Loads

- In this case a DR scheme is proposed where the MGO can issue a control signal P_{max} to the load entity. The demand model developed earlier and integrated into the operations scheduling model of the microgrid, is used to extract an optimal value of the control signal P_{max} for the specific temperature and price structure. The effect of this control signal on the controllable load profile of the microgrid system has been studied in this case.

4.3.2 Case Studies

The proposed model incorporates temperature and TOU pricing data as input parameters to the optimization framework. The temperature and TOU pricing data corresponding to a particular summer day in June 2012, in Ontario, Canada is shown in Figure. 4.2.

The summer TOU pricing scheme comprises three price steps, 0.042 \$/kWh, 0.076 \$/kWh and 0.091 \$/kWh corresponding to the off-peak, mid-peak and peak hours of the day, respectively. The average temperature on this particular day was 19.6 °C.

The base load, which exceeds both the controlled and uncontrolled load components has been used in accordance with the microgrid load characteristics. The base load profile over 24 hours is shown in Figure. 4.3.

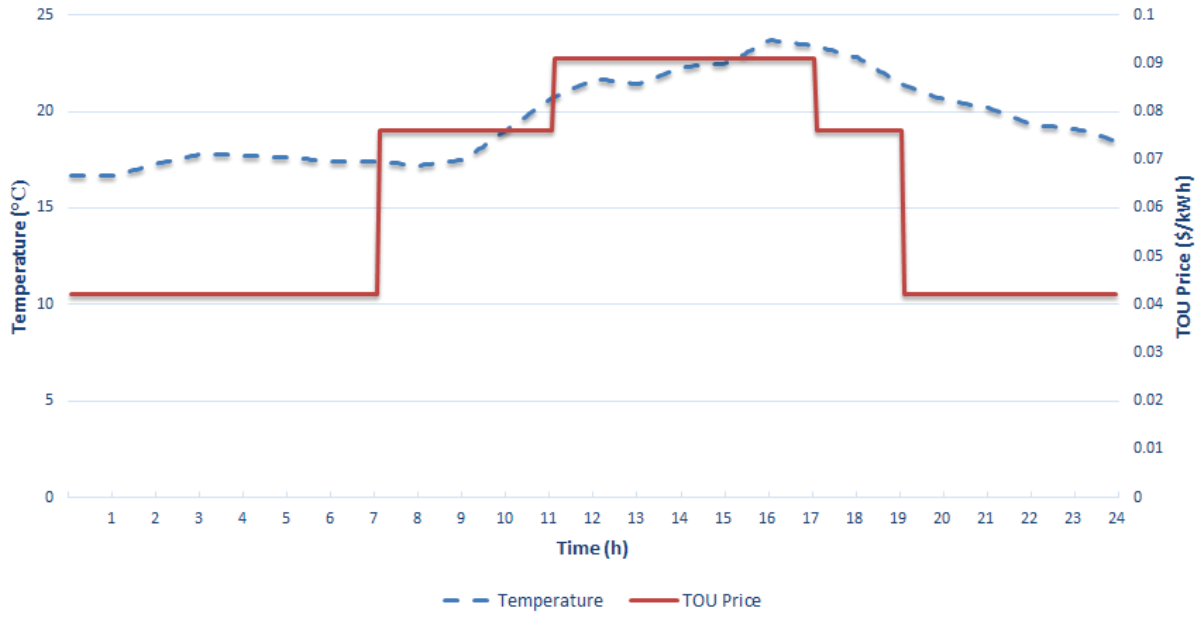

Figure 4.2: Temperature and TOU pricing profile.

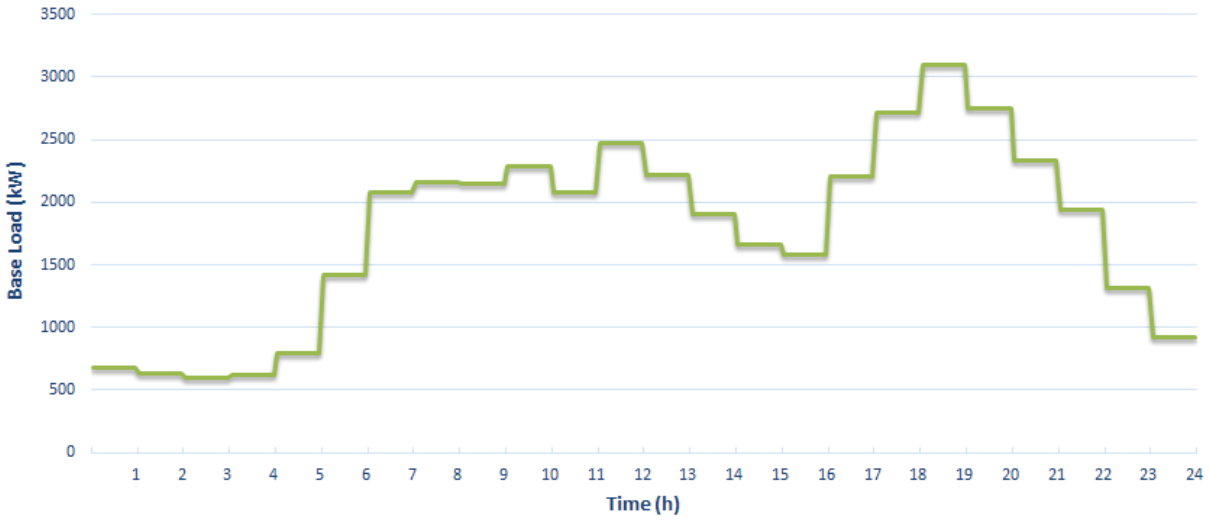

Figure 4.3: Base load profile of residential customers in a microgrid.

Figure 4.4 and 4.5 show the PV generation profile and the assumed wind generation profile for the same day under consideration, respectively. Uncertainties in PV and wind generation have not been considered. Instead, the wind generation output and PV output are considered to be exogenously fed to the system. The generation profile of the PV panels and the wind turbine have been included with due consideration of the capacity limits of the individual units in the microgrid.

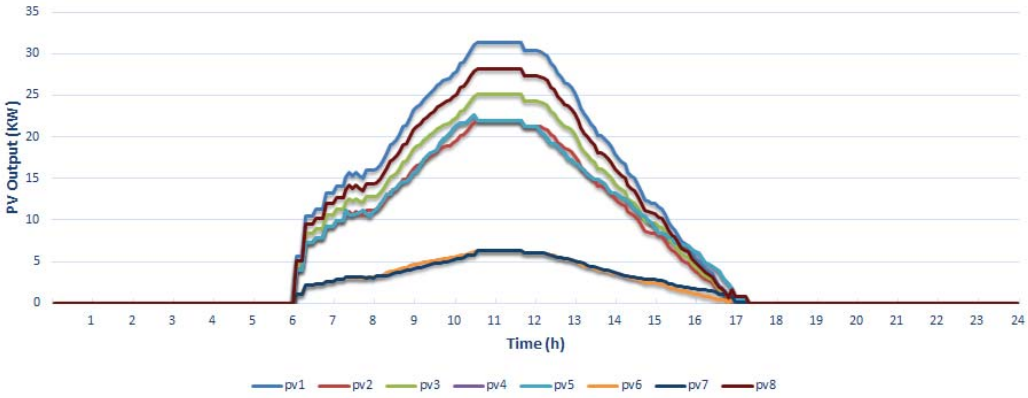

Figure 4.4: PV generation profile.

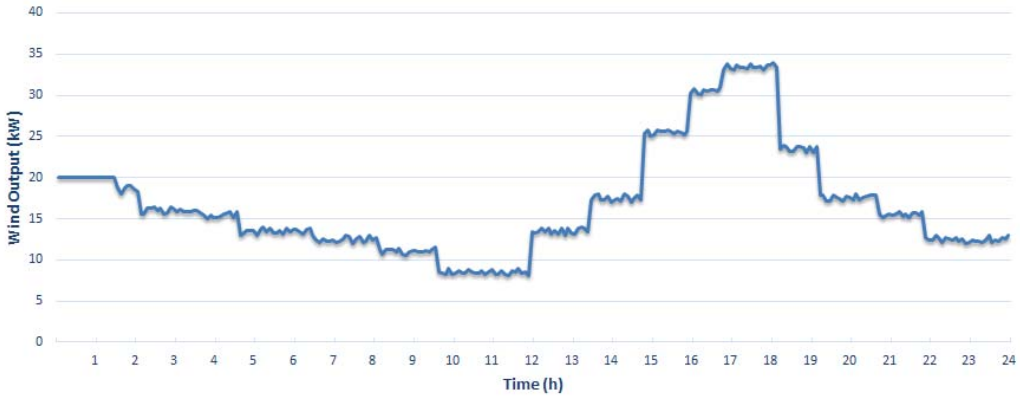

Figure 4.5: Wind generation profile.

It is to be noted that in the results below, subscripts nc and c have been used to denote the uncontrolled load case (Case 1) and controlled load case (Case 2), respectively.

Case 1:

In this case, the load is not influenced by any control signal from the MGO. The load in this case is a function of the temperature and TOU price only. The base load and the neural network estimated uncontrolled load as a constituent of the total system load is

shown in Figure. 4.6. It can be seen that the shift in the load profile of the uncontrolled load across the time period has a correlation with the TOU price signal while the magnitude of load variation is determined by its relation to the external temperature as modeled by the neural network.

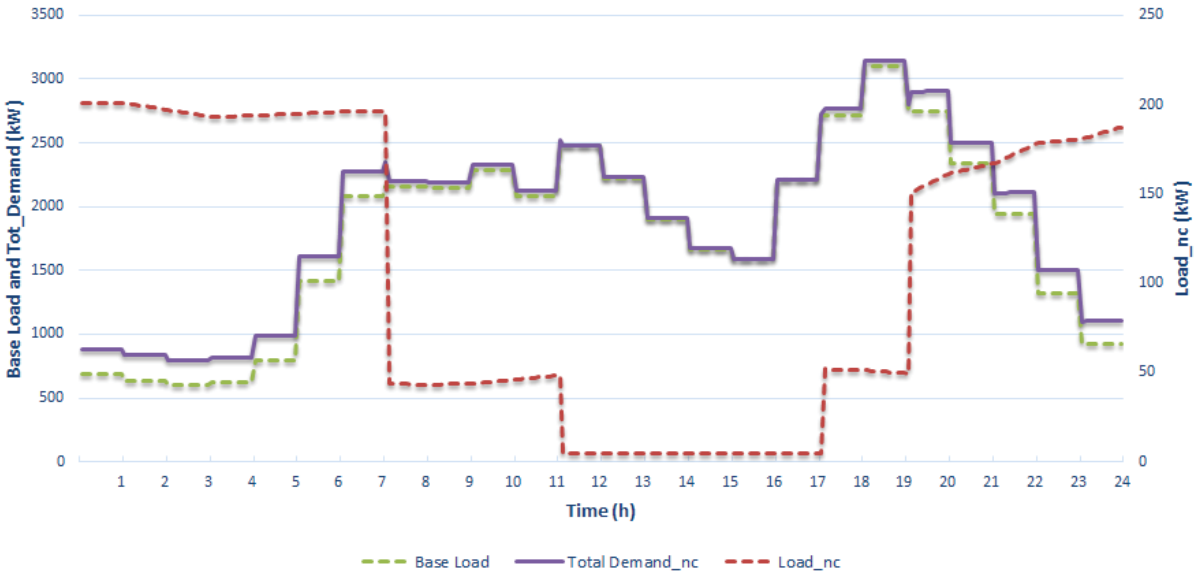

Figure 4.6: Cumulative load profile, base load and uncontrollable load in Case 1.

Figure 4.7 shows the optimal diesel generation schedule as an outcome of the cost minimization optimization. The generators $G2\_nc$ and $G3\_nc$ from Figure. 4.7 correspond to the CHP diesel and gas turbine units at bus 9 and 13 respectively, while $G1\_nc$ corresponds to the main diesel generator unit at bus 1. The dispatch in Figure.4.7 is in line with the cost characteristic and generation constraints of the concerned generators. It has to be noted that, $G2\_nc$ and $G3\_nc$ being the cheapest generation sources in the microgrid, operate at their full potential during the scheduling period.

Figure 4.8 shows the cumulative ESS discharge and charging profile during the off-peak pricing hours. Here, $Tot\_ch - nc$ and $Tot\_dch - nc$ describe the power charged and discharged for all ESS devices in the uncontrolled load case (Case 1). As described in the objective function, the MGO makes a savings in generation cost when the ESS batteries discharge and it pays a price equivalent to cost of supplying the load when it is charging. Figure 4.9 depicts the ESS discharge and charging profile during peak demand cycle. The ESS operation is optimized such that it charges when the cost of supplying

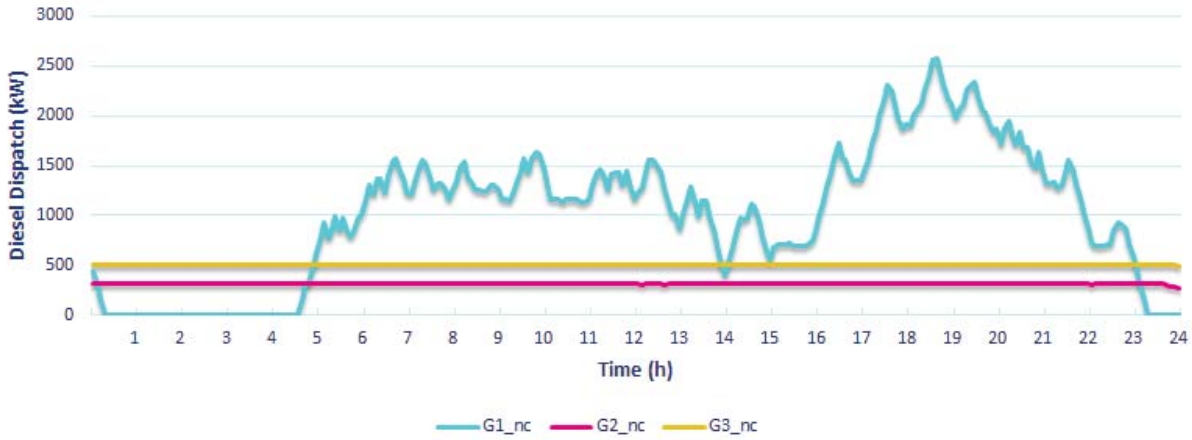

Figure 4.7: Optimal generation dispatch in Case 1.

the load is low (low TOU prices) and maximizes the discharge during the peak TOU price periods. The total energy charged by the ESS during the off-peak hours is 4.5 MWh and the energy discharged is 2.8 MWh. Similarly, the total energy charged by the ESS during the peak period is 1.4 MWh and the total energy discharged during this period is 3 MWh respectively.

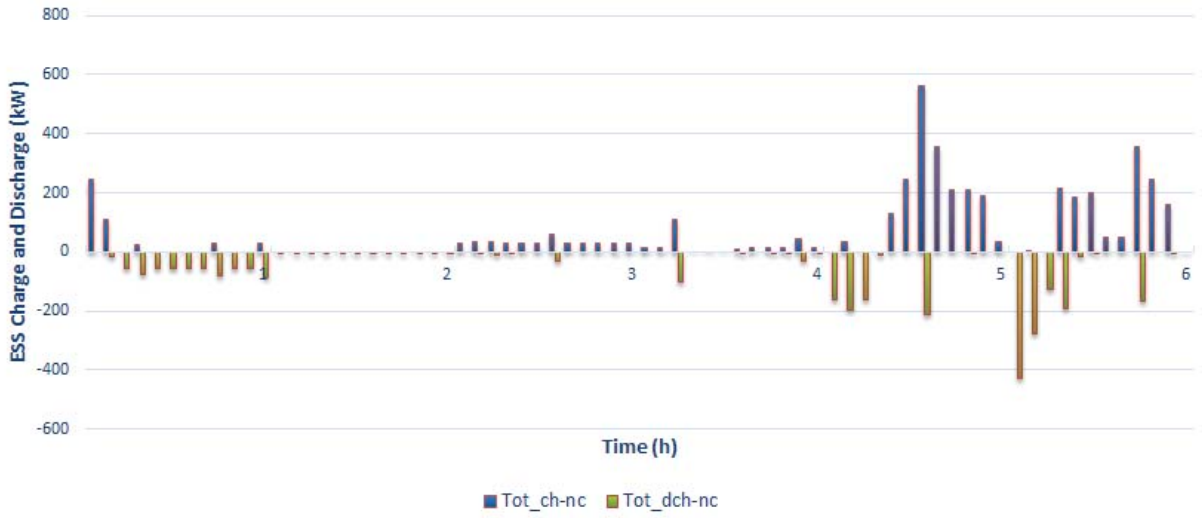

Figure 4.8: ESS dispatch during off-peak in Case 1.

Case 2:

In this case, the controllable load is influenced by the MGO imposed control signal

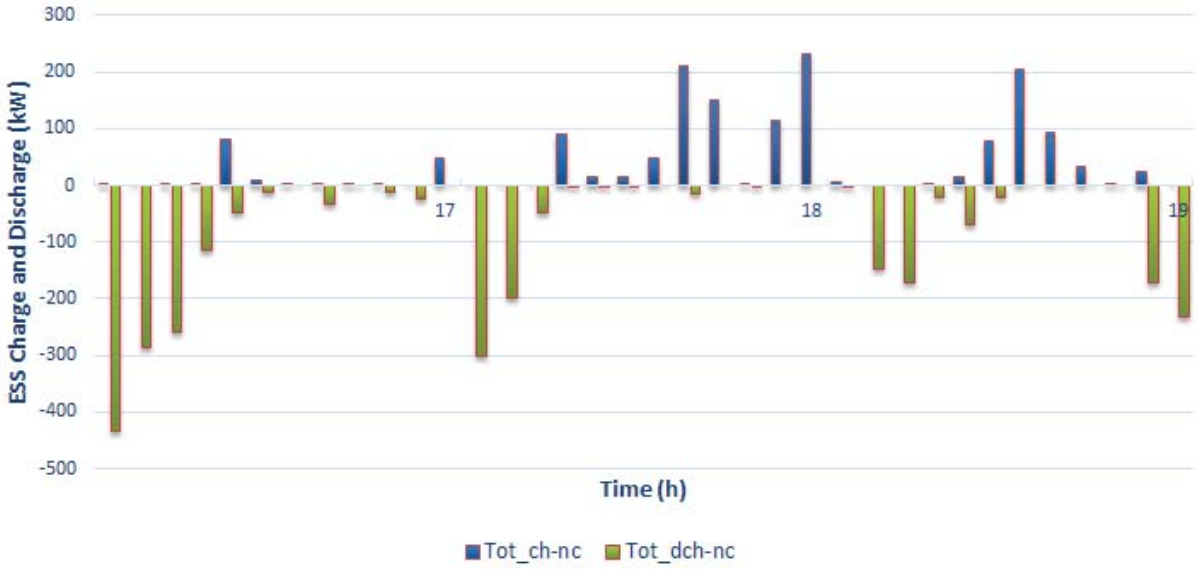

Figure 4.9: ESS dispatch during peak in case 1.

P_{max}. The effect of P_{max} on the controllable load and the generation schedule are presented alongside a comparative study with Case 1. The controllable load profile under an active control signal P_{max} and its comparison with the uncontrolled load in Case 1 is discussed.

Figure 4.10 shows small perturbations in the controlled load profile during the period corresponding to TOU price of 0.042 \$/kWh where the load experiences a shift which is reflected by the generation shift and the subsequent perturbations in the sigmoid function in optimization. A reduction in the load profile is also observed when subjected to a control by the MGO. The total reduction in load energy over the scheduling period accounts for 1620 kWh which corresponds to 5% reduction of controllable load energy in comparison to the case where the load is not externally controlled (Case 1). To better demonstrate the load variation, a section of the demand profile during a selected off-peak and peak intervals are shown in Figure. 4.11 and 4.12 respectively. Significant demand reductions from the MGO's perspective is noted, with the control signal, as against the uncontrolled load behavior. It is to be notd from Figure. 4.11 and 4.12 that the amount of load reduction on the system demand is significant during the off-peak periods as against the peak TOU price periods. It is due to the fact that the quantum of controllable loads presented to the LPE during the peak TOU price were negligible which was reflected in the load model from the LPE as represented in Figure. 3.5. Thus, the scope of controllable load reduction

during the peak period is restricted as illustrated in Figure. 4.12.

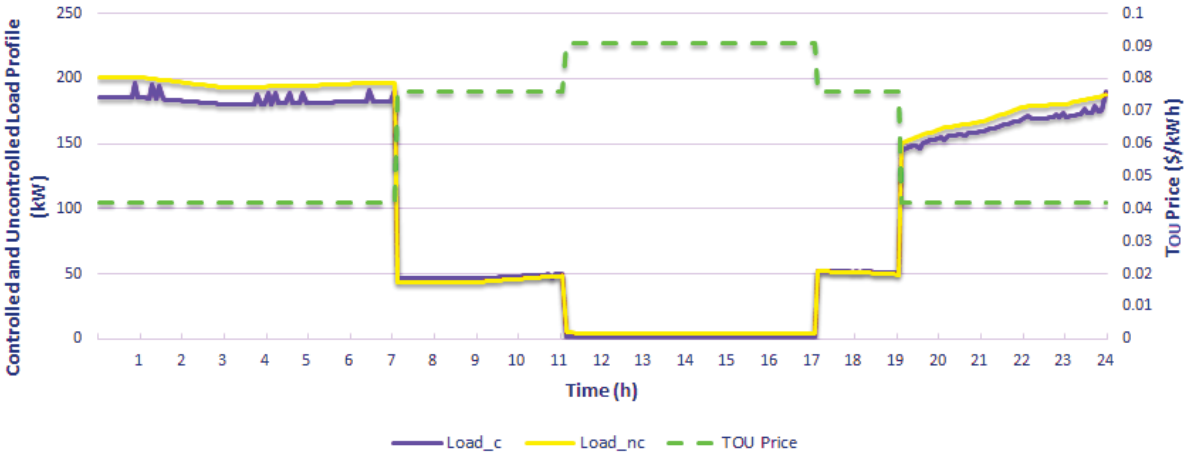

Figure 4.10: Comparison of controlled and uncontrolled load profile in Case 1 and 2.

The change in load profile is accompanied by a change in diesel dispatch and the ESS output, as shown in the figures next. Figure 4.13 depicts the optimal generation profile of the diesel generators for Case 2.

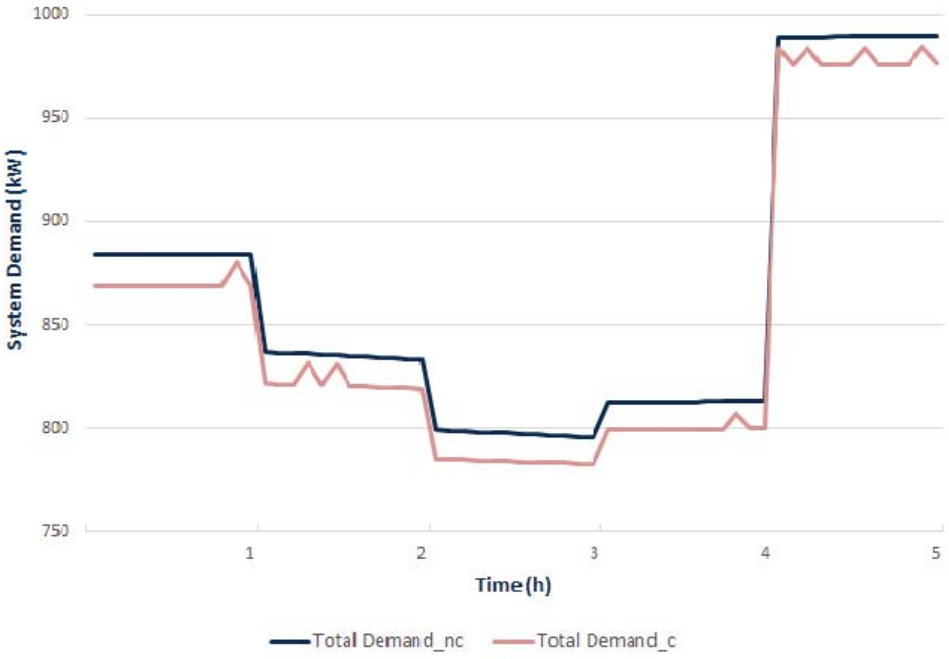

Figure 4.11: Effect of P_{max} on the system demand for a selected off-peak interval.

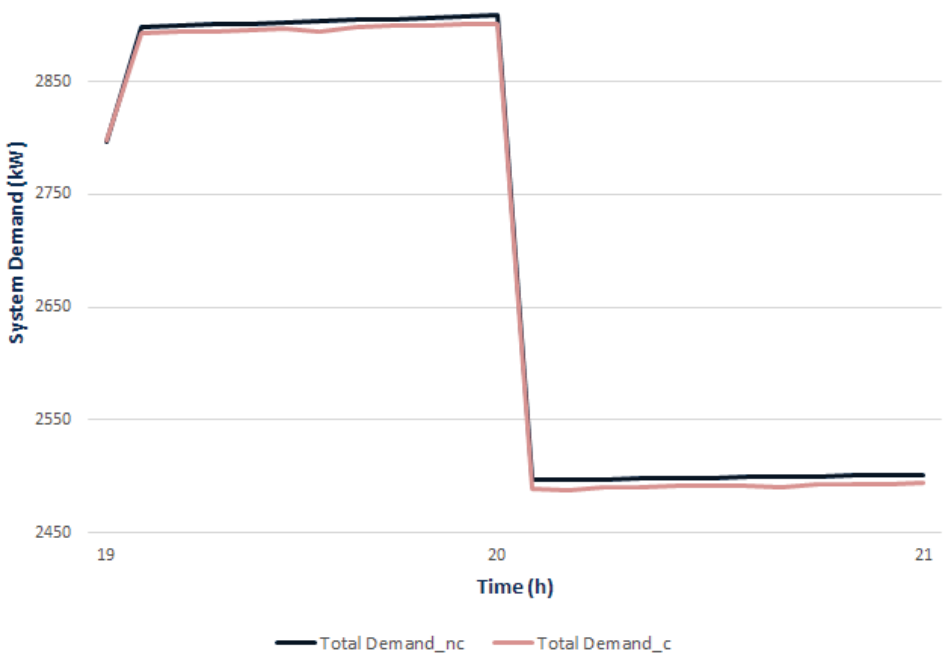

Figure 4.12: Effect of P_{max} on the system demand for a selected peak interval.

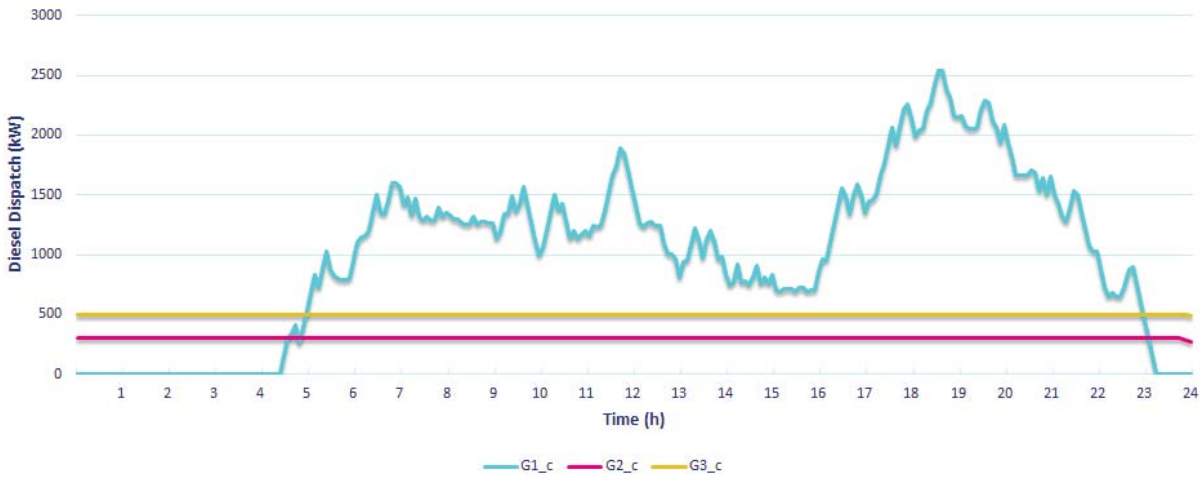

Figure 4.13: Optimal generation dispatch in Case 2.

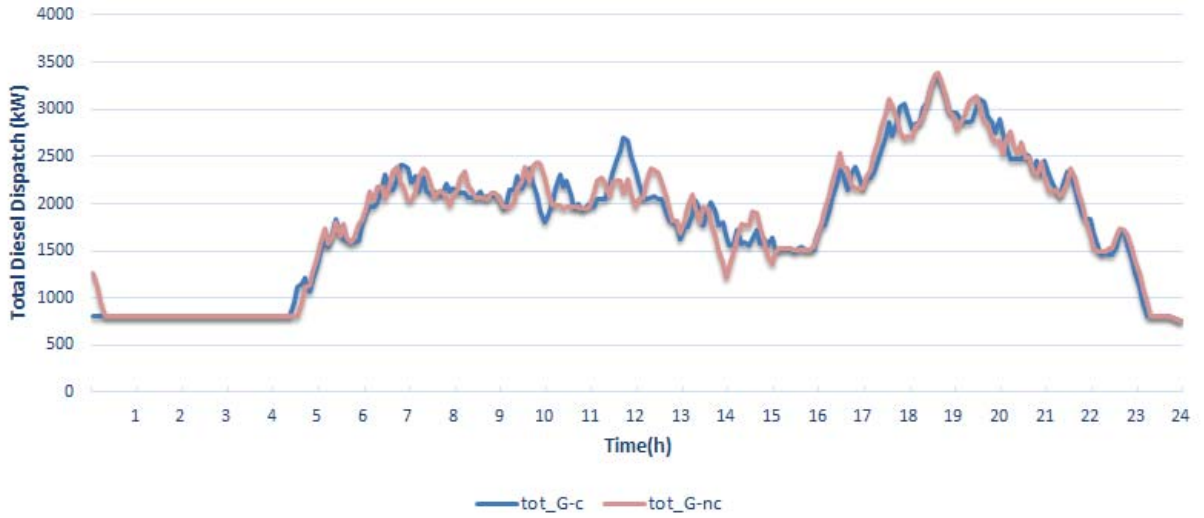

Figure 4.14: A comparison of diesel generator dispatch under Case 1 and 2.

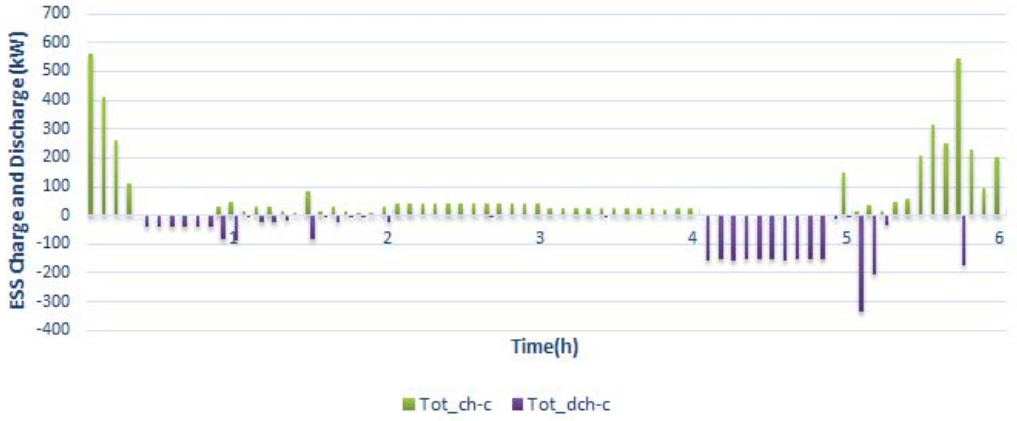

Figure 4.15: ESS dispatch during off-peak in Case 2.

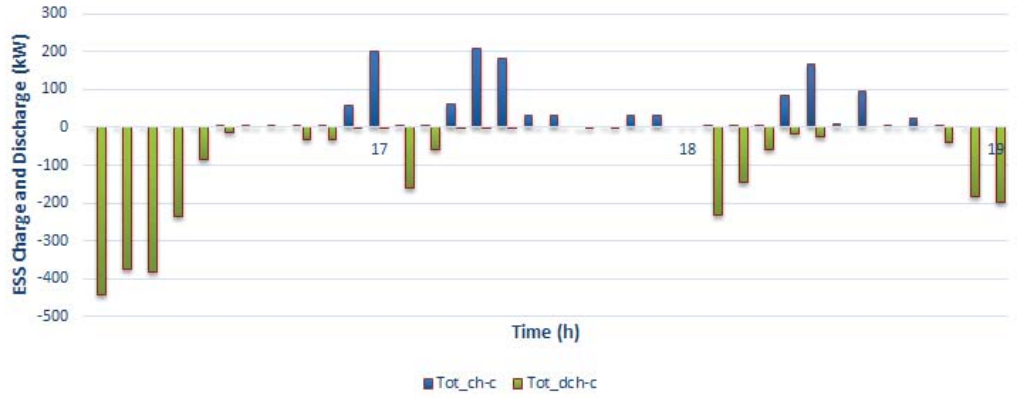

Figure 4.16: ESS dispatch during peak in Case 2.

Referring to Figure. 4.14, tot_G-c and tot_G-nc represent the cumulative generation profile considering three conventional diesel generators. Figure 4.14 shows the variation in the diesel generator dispatch profile in Case 1 and the controllable load case (Case 2). It is noted that a total energy of 1,821 kWh from diesel generators is conserved under Case 2 as against Case 1 under the same scheduling period. Similar to Case 1, the ESS dispatch under off-peak and peak periods have been shown in Figure. 4.15 and 4.16 respectively. The total charging energy of the combined ESS with controllable loads is 14.5 MWh which is 544 kWh less than the energy consumed in the uncontrolled load case (Case 1). The total energy discharged in Case 2 is equal to 14 MWh, which is significantly lower than the uncontrolled load case discharge owing to the reduced demand requirements. Absolute difference between the ESS dispatch at each instant over the two cases is shown in Figure. 4.17.

A 5% reduction in the controllable load is not insignificant when the cost components of the system are taken into account. It is estimated that for this specific day under study, total savings of $560 can be achieved for the MGO taking into account the complete cost characteristics of the microgrid, while the projected yearly savings is $204,388; which is a significant saving considering the size and the scope of isolated microgrids (Table 4.2). It is also noted from Table 4.3 that the total DR related energy savings achieved for the day is 3,008 kWh which can be projected to 1,098 MWh annually, which is quite significant.

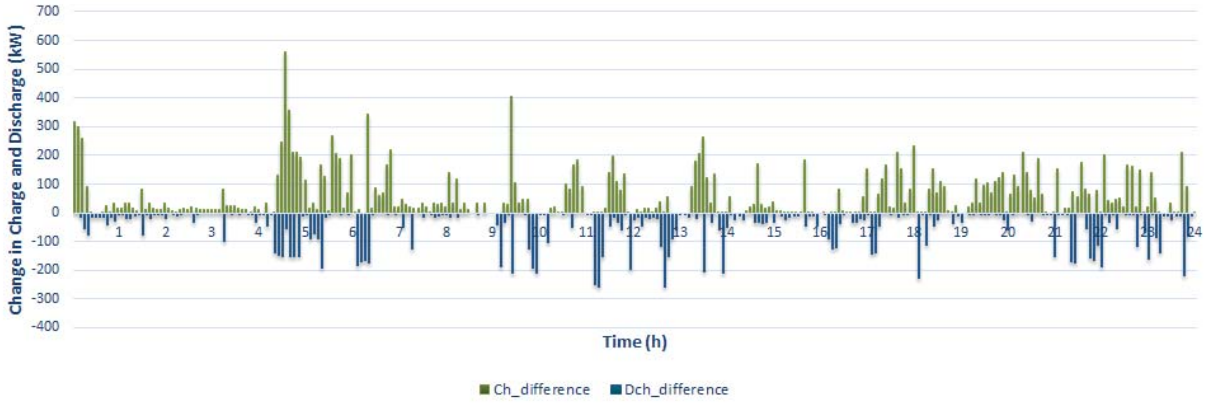

Figure 4.17: Absolute change in ESS dispatch.

Table 4.2: Comparison of costs between Case 1 and Case 2.

	Diesel Dispatch Cost ($)	ESS Charging Cost ($)	Savings from ESS Discharge ($)	Total Cost ($)	Savings ($/year)
Case 1	105,730	824	914	105,640	204,388
Case 2	105,207	780	907	105,080	

Table 4.3: Energy dispatch comparison between Case 1 and Case 2.

	Diesel Generation (kWh)	ESS Charging (kWh)	ESS Discharging (kWh)	Demand Response (kWh)
Case 1	524,478	15,057	15,520	-
Case 2	522,658	14,513	14,876	3,008

4.3.3 Inclusion of Constant Energy Constraint

In any system, while the DR program may try to reduce the peak demand, the customer actually intends to shift the consumption to off-peak periods. Therefore, without compromising on the operational duration and total energy consumption of the individual

appliances, the energy is paid back to the off-peak hours. In the MEMS model discussed earlier, reduction of the controllable load under the influence of P_{max} has been the forcing function of the DR. Cost minimization based generation scheduling resulted in a reduction of the load in an effort to minimize the cost. While cost minimization of microgrid operations achieved its objective, the significance of load shift was not considered.

In order to take into consideration the DR effects across the operating horizon, the MEMS model is modified to include a constant energy constraint. The objective function is modified to reflect the effect of TOU prices on the controllable demand.

Objective Function

$$J = \sum_{g}\sum_{t}(ax_g v_{g,t} + bx_g P_{g,t} + SUC_g y_{g,t} + SDC_g z_{g,t}) + \sum_{ba}\sum_{t}(TOU_t P^{ch}_{ba,t} ch_{ba,t} - TOU_t P^{dch}_{ba,t} dch_{ba,t}) + \sum_{t}(Pd^e_t TOU_t) \quad (4.1)$$

where the last term of (4.1) denotes the total customer payment, which is a function of the controlled demand.

Constant Energy Constraint

$$\sum_{t} Pd^e_t \geq Total_{Energy} \quad (4.2)$$

Energy is conserved in this case and the load is shifted across the scheduling period. The total demand profile and the load shift is depicted in Figure. 4.18.

The total demand as depicted in the figure is a summation of the controllable load and system base load. As seen in Figure. 4.18, the demand that has been substantially reduced during the peak hours is effectively shifted to the off-peak periods. The maximum instantaneous demand has been reduced from 3,147 kW to 3,095 kW and the energy consumption during the peak hours has reduced by 1,508 kWh.

4.4 Computational Performance

The proposed MEMS model has been executed on GAMS [38], the DICOPT [39] solver was used to solve the MINLP problem. The MILP master problem was assigned to CPLEX [40] solver and the NLP subproblems were assigned to SNOPT [41] solver. The solution statistics are listed below:

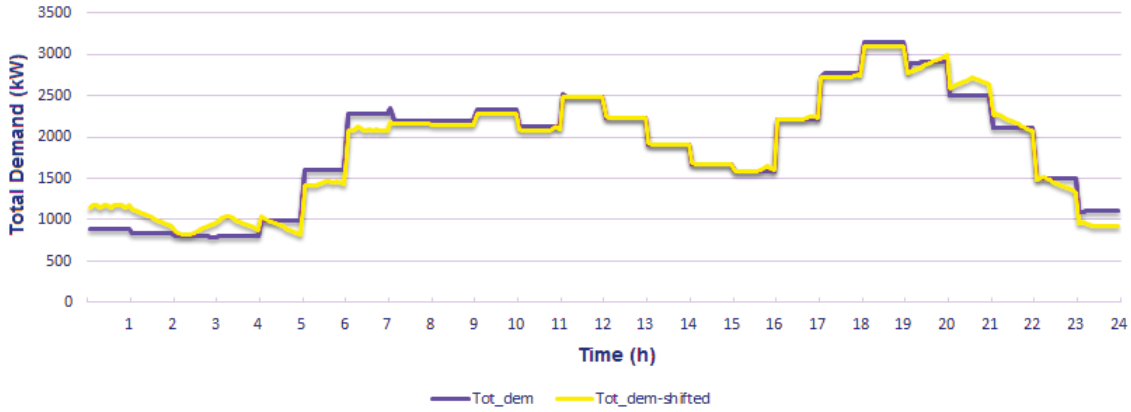

Figure 4.18: Controllable load shift profile.

- Number of equations: **28,910**
- Number of variables: **18,721**
- Number of nonlinear non-zeros: **10,368**
- Number of discrete variables: **7,200**
- CPU time: **574.01** sec

4.5 Summary

This chapter brought to light the CIGRE microgrid test system to test the effectiveness of the optimal DR model under the system's isolated mode of operation. The mathematical models of DR was analyzed considering different case studies. The effect of controlling signal on DR and the subsequent variation in generation scheduling has been examined. The total energy conservation and the resultant savings for the MGo have also been highlighted. Load shifting of controllable demand based on TOU and its effect on peak reduction has also been demonstrated.

Chapter 5

Conclusions and Future Work

5.1 Summary and Conclusions

Chapter 1 presented the main motivations behind this research. The motivations brought to light the need for a novel DR scheme and its implementation on a smart microgrid framework. A literature review of related works on DR with emphasis on microgrid based DR schemes were presented. This chapter also highlighted the research objectives of this thesis.

Chapter 2 presented a brief background of the tools and models of this research. An overview of DR and microgrids was presented to illustrate their significance and associated characteristics. General estimation techniques and modeling procedures along with a background on load modeling using neural networks were also presented. This chapter also outlined the mathematical problem of the UC and elaborated on the optimization methods and tools used in this research.

In Chapter 3, a detailed mathematical model that incorporates DR within an optimization framework was proposed. An architecture of the proposed DR model was presented while illustrating its individual components. A detailed mathematical model of MEMS was developed and it was followed by a load estimation technique incorporated into the LPE. Neural network based supervised learning technique was used to simulate a functional relation between complex physical parameters. A TOU based dynamic pricing scheme, outside temperature and MGO imposed maximum limit P_{max} on load was used to model load consumption of an EHMS house during the summer months in Ontario.

The chapter concludes by providing the resultant mathematical model of the MEMS with neural network-microgrid integration which performs the optimal scheduling of generation resources of a microgrid.

In Chapter 4, a controlling scheme of DR through MGO was investigated on a CIGRE microgrid system. Case studies were carried out to better demonstrate the effect of the proposed model on energy management in microgrids. Cost based optimization of the neural network integrated model was performed and the effect of the control signal P_{max} on the two cases were shown. The total load conservation with and without the controlling scheme and the resultant savings for the MGO were presented to shown the effectiveness of the proposed optimal DR model. A separate analysis of the DR model with energy payback was presented to reflect the real-world customer behavior in a microgrid system.

The proposed system does not compromise on the operational privacy of the individual users in a power system set up. In essence, the control scheme solely considers the operational data available at the supply end and proceeds to reduce the peak consumption. The proposed model proves to be effective under practical constraints where the MGO is not expected to have a complete knowledge of the operating status of individual devices under operation. Further, the mathematical model formulated in this work belongs to a class of MINLP problems. This complex NP hard problem has been solved using commercial solvers with guaranteed precision. The resource constraints and the execution time encountered while solving this model seem to fit well under most practical scenarios.

5.2 Contributions

The main contributions made of this thesis are summarized as follows:

- A detailed mathematical model demonstrating the fundamental governing relationship between the outside temperature, TOU price and maximum demand limit (P_{max}) on the controlled load was presented. This model was estimated using neural network which was trained by supervised learning.
- A comprehensive cost minimization based generation scheduling model for an isolated microgrid has been developed. Diesel generators, ESS devices, PV and wind turbines have been considered for the studies.

- The novel controlled load model is integrated with the microgrid operations model to formulate the MEMS model. The effect of MGO's control signal P_{max} is examined on the demand reduction of the controllable load and the cost savings have been clearly illustrated.

- The proposed model was validated under realistic test cases and a comparative analyses was made with the base case. Besides the MGO based cost minimization approach, a customer payback model incorporated into the developed DR problem was studied.

5.3 Future Work

Possible future work as a continuation of the present research are as follows:

- The proposed optimal DR model could be extended by modeling the system load as a function of voltage. The present model while considering a least cost dispatch, does not emphasize on system security. Additional voltage control of the load will produce a security constrained optimal DR which will be effective from the perspective of isolated microgrid.

- The proposed controllable load modeling of the system was based on the supervised learning technique, the goodness of which depends to a large extent on the quality and the quantity of the historical data. Reinforcement learning based modeling of the controllable load that adapts to the system behavior and relearns the model could be used in the future.

Bibliography

[1] "FERC."https://www.ferc.gov/legal/staff-reports/12-20-12-demand-response.pdf, 2012.

[2] "Blueprint for demand response in Ontario." http://sites.energetics.com/madri/toolbox/pdfs/ontario/blueprint.pdf, 2012.

[3] I.H.Rowlands, "Demand Response in Ontario," https://www.ieso.ca/imoweb/pubs/marketreports/omo/2009/demand_respose.pdf.

[4] "Senate Bill on Demand Response." http://www.cga.ct.gov/2012/act/pa/pdf/2012PA-00148-R00SB-00023-PA.pdf, 2012.

[5] A. Sinha, S. Neogi, R. Lahiri, S. Chowdhury, S. Chowdhury, and N. Chakraborty, "Smart grid initiative for power distribution utility in India," in *Proc. IEEE Power and Energy Society General Meeting, 2011.*

[6] A. Ipakchi and F. Albuyeh, "Grid of the future," *IEEE Power and Energy Magazine*, vol. 7, no. 2, pp. 52–62, 2009.

[7] "NSERC Smart Microgrid Network." http://www.smart-microgrid.ca/.

[8] N. Hatziargyriou, H. Asano, R. Iravani, and C. Marnay, "Microgrids," *IEEE Power and Energy Magazine*, vol. 5, no. 4, pp. 78–94, 2007.

[9] K.-H. Ng and G. B. Sheble, "Direct load control-a profit-based load management using linear programming," *IEEE Transactions on Power Systems*, vol. 13, no. 2, pp. 688–694, 1998.

[10] C. Kurucz, D. Brandt, and S. Sim, "A linear programming model for reducing system peak through customer load control programs," *IEEE Transactions on Power Systems*, vol. 11, no. 4, pp. 1817–1824, 1996.

[11] N. Ruiz, I. Cobelo, and J. Oyarzabal, "A direct load control model for virtual power plant management," *IEEE Transactions on Power Systems*, vol. 24, no. 2, pp. 959–966, 2009.

[12] H. Mohsenian-Rad and A. Leon-Garcia,"Optimal residential load control with price prediction in real-time electricity pricing environments,"*IEEE Transactions on Smart Grid*, vol. 1, no. 2,pp. 120–133, 2010.

[13] T. Logenthiran, D. Srinivasan, A. M. Khambadkone, and H. N. Aung, "Multiagent system for real-time operation of a microgrid in real-time digital simulator," *IEEE Transactions on Smart Grid*, vol. 3, no. 2, pp. 925–933, 2012.

[14] L. P. Qian, Y. J. A. Zhang, J. Huang, and Y. Wu, "Demand response management via real-time electricity price control in smart grids," *IEEE Journal on Selected Areas in Communications*, vol. 31, no. 7, pp. 1268–1280, 2013.

[15] F. C. Schweppe, R. D. Tabors, M. Caraminis, and R. E. Bohn, "Homeostatic utilty control," *IEEE Transactions on Power Apparatus and Systems*, vol. 99, no. 3, 1980.

[16] Y. Ozturk, D. Senthilkumar, S. Kumar, and G. Lee, "An intelligent home energy management system to improve demand response," *IEEE Transactions on Smart Grid*, vol. 4,no, 2, 2013.

[17] F. Katiraei, R. Iravani, N. Hatziargyriou, and A. Dimeas, "Microgrids management," *IEEE Power and Energy Magazine*, vol. 6, no. 3, pp. 54–65, 2008.

[18] H. Kumar Nunna and S. Doolla, "Energy management in microgrids using demand response and distributed storage a multiagent approach," *IEEE Transactions on Power Delivery*, vol. 28, no. 2, 2013.

[19] B. Jiang and Y. Fei, "Dynamic residential demand response and distributed generation management in smart microgrid with hierarchical agents," in *Proc. Int. Conf. on Smart Grid and Clean Energy Technologies*, 2011.

[20] D. O'Neill, M. Levorato, A. Goldsmith, and U. Mitra, "Residential demand response using reinforcement learning," in *First IEEE International Conference on Smart Grid Communications (SmartGridComm), 2010*, pp. 409–414, IEEE, 2010.

[21] M. Arriaga, C.A. Cañizares and M. Kazerani,"Renewable energy alternatives for remote communities in Northern Ontario, Canada," in *IEEE Transactions on Sustainable Energy*, vol. 4, no. 3, pp. 661–670, 2013.

[22] S. Wong, "Microgrid research activities in Canada," in *Presentation at Jeju 2011 Symposium on Microgrids*, `http://der.lbl.gov/sites/der.lbl.gov/files/jeju_wong.pdf`, 2011.

[23] M. Z. Kamh, R. Iravani, and T. H. El-Fouly, "Realizing a smart microgrid pioneer Canadian experience," in *Proc. IEEE Power and Energy Society General Meeting, 2012, San Diego, CA, USA*.

[24] M. H. Albadi and E. El-Saadany, "A summary of demand response in electricity markets," *Electric Power Systems Research*, vol. 78, no. 11, pp. 1989–1996, 2008.

[25] FERC, "Grid 2030 a national vision for electricity second 100 years." `https://www.ferc.gov/eventcalendar/Files/20050608125055-grid-2030.pdf`, 2003.

[26] USA. Department Of Energy, "U.S. Department of Energy's Ressearch and Development on Microgrid." `http://der.lbl.gov/sites/der.lbl.gov/files/Smith_2010.pdf`, 2010.

[27] J. V. Beck and K. J. Arnold, "Parameter estimation in engineering and science," *Wiley, New York*, 1977.

[28] A. Ng, "Machine learning." `http://cs229.stanford.edu/notes/cs229-notes1.pdf`, 2012.

[29] K. Hornik, M. Stinchcombe, and H. White, "Multilayer feedforward networks are universal approximators," *Journal on Neural Networks*, vol. 2, no. 5, pp. 359–366, 1989.

[30] F. Scarselli and A. Chung Tsoi, "Universal approximation using feedforward neural networks: A survey of some existing methods, and some new results," *Journal on Neural Networks*, vol. 11, no. 1, pp. 15–37, 1998.

[31] Zhang, Q. Jun and Gupta, C. Kuldip, "Neural Network Structure," http://www.ieee.cz/knihovna/Zhang/Zhang100-ch03.pdf.

[32] M. Beale, M. T. Hagan, and H. B. Demuth, "Neural network toolbox," *Neural Network Toolbox, The Math Works*, pp. 5–25, 1992.

[33] J. M. Arroyo and A. J. Conejo, "Optimal response of a thermal unit to an electricity spot market," *IEEE Transactions on Power Systems*, vol. 15, no. 3, pp. 1098–1104, 2000.

[34] G. L. Nemhauser and L. A. Wolsey, *Integer and combinatorial optimization*, vol. 18. Wiley New York, 1988.

[35] "Branch and bound." http://www.stanford.edu/class/ee364b/notes/bb_notes.pdf, 2007.

[36] J. Clausen, "Branch and bound algorithms-principles and examples," *Department of Computer Science, University of Copenhagen*, pp. 1–30, 1999. http://janders.eecg.toronto.edu/1387/readings/b_and_b.pdf

[37] "Optimization." http://www.math.bme.hu/~bog/GlobOpt/Chapter5.pdf.

[38] "GAMS." http://www.gams.com/.

[39] "DICOPT." http://www.gams.com/dd/docs/solvers/dicopt.pdf, 2007.

[40] "CPLEX." http://http://www.gams.com/dd/docs/solvers/cplex.pdf.

[41] "SNOPT." http://www.gams.com/dd/docs/solvers/snopt.pdf.

[42] "MATLAB." http://www.mathworks.com/.

[43] K. Rudion, A. Orths, Z. Styczynski, and K. Strunz, "Design of benchmark of medium voltage distribution network for investigation of DG integration," *Proc. IEEE Power Engineering Society General Meeting, 2006*, Montreal, Canada.

.